Supplement of Atmos. Chem. Phys., 18, 12433–12460, 2018
https://doi.org/10.5194/acp-18-12433-2018-supplement

Atmospheric Chemistry and Physics
Open Access
EGU

Supplement of

Constraining nucleation, condensation, and chemistry in oxidation flow reactors using size-distribution measurements and aerosol microphysical modeling

Anna L. Hodshire et al.

Correspondence to: Anna L. Hodshire (hodshire@rams.colostate.edu)

S1. GoAmazon2014/5 SMPS-derived volume exposures and mean diurnal cycle of monoterpenes and isoprene

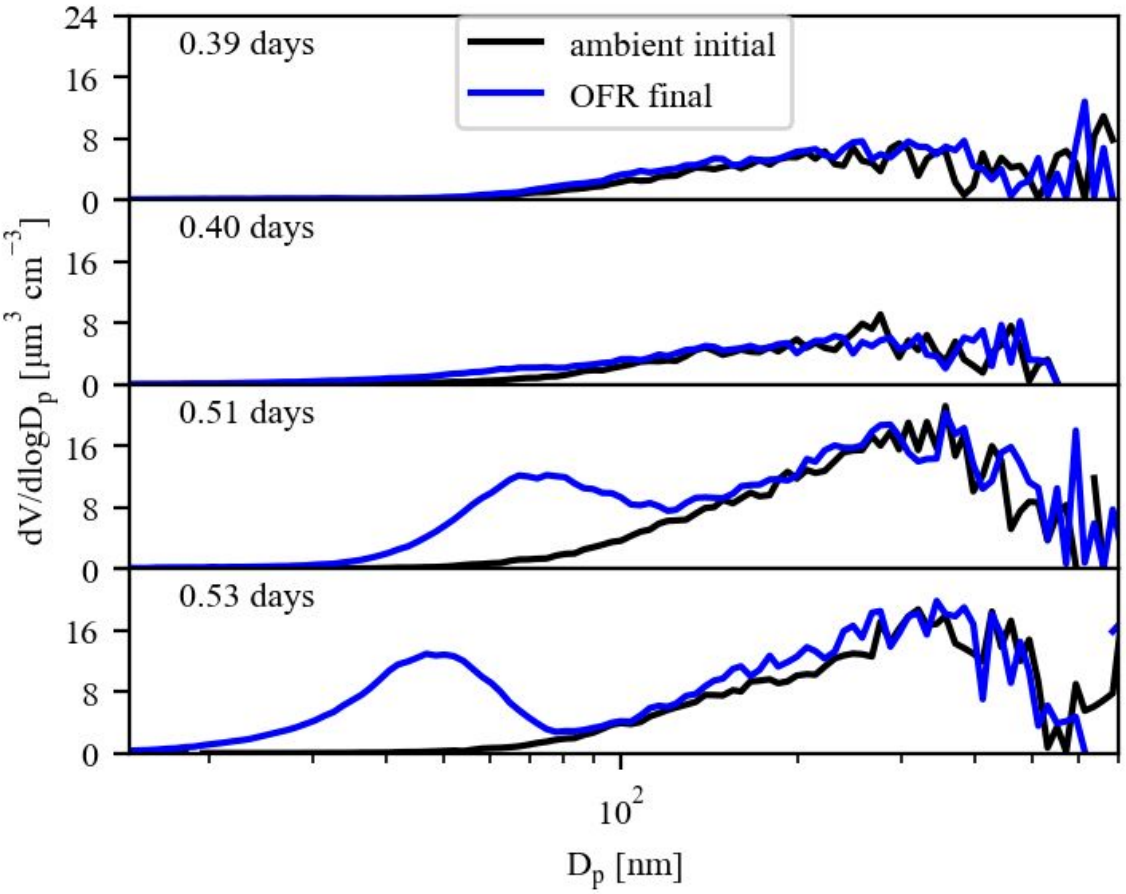

Figure S1. GoAmazon initial (i.e. ambient air, black line) and final (i.e. after OFR processing, blue line) SMPS-derived volume distributions for each individual exposure modelled in this study. The differences in SOA production between exposures of similar ages are due to the fact that the exposures were taken from different times during the campaign and thus different precursor concentrations were present (Table 2).

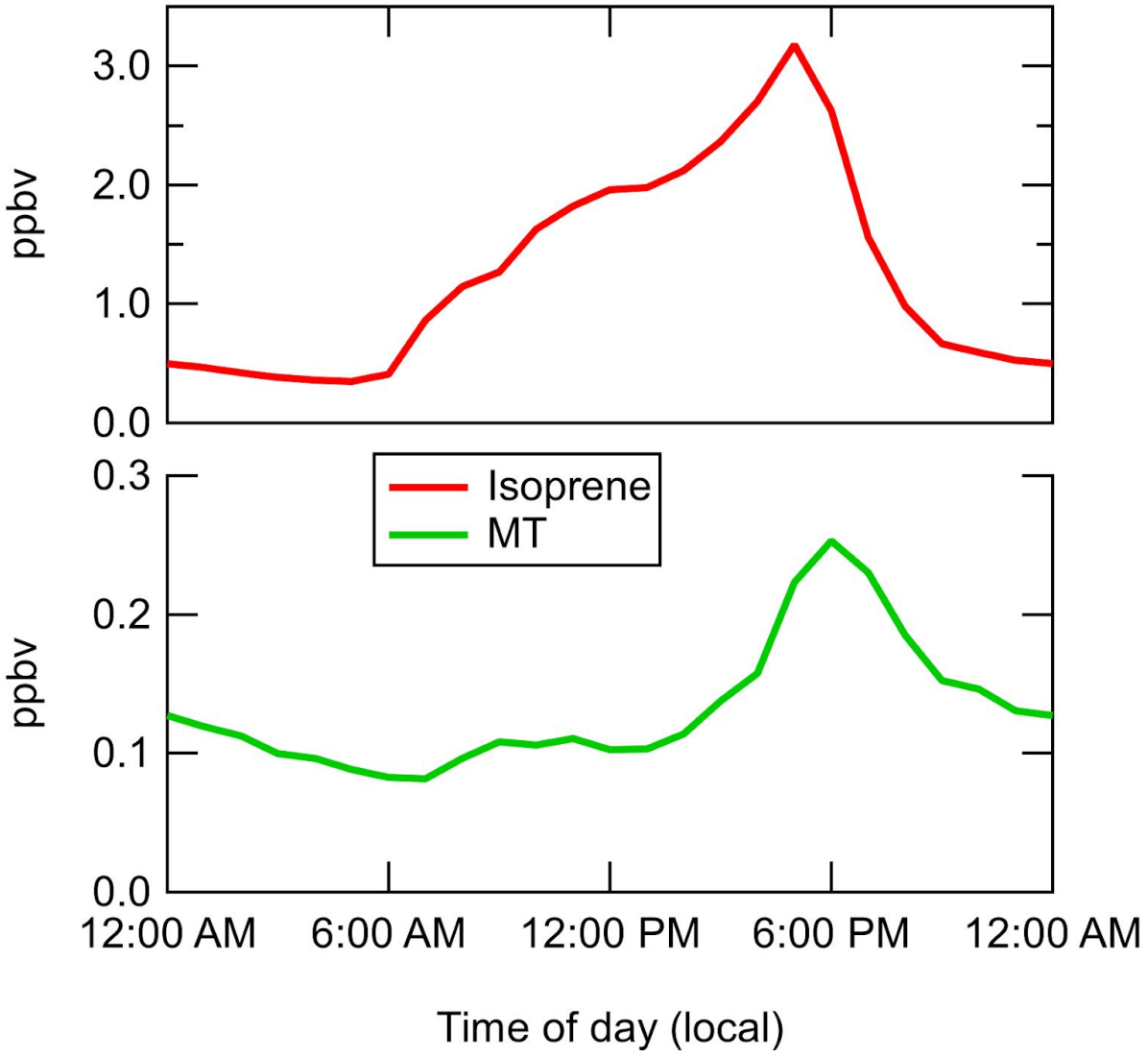

Figure S2. The mean observed diurnal cycle of isoprene (red line) and monoterpenes (MT; green line) for the dry season during the GoAmazon2014/5 campaign.

S2. BEACHON-RoMBAS individual exposures and best/worst case distributions

The following are the individual representations of the model simulations for each BEACHON-RoMBAS exposure modelled in this study. Figures S3, S5, S7, S9, S11, S13, S15, and S17 give the normalized mean error (NME) values for the parameter space that lies within (Table 3) the NUC1 nucleation scheme and base value of the reactive uptake coefficient. Figures S4, S6, S8, S10, S12, S14, S16, and S18 plot each observed final moment (solid black lines) used in computing the NME statistic (number, diameter, surface area, and volume) compared to the six TOMAS cases with the lowest (best) NME statistic (solid colored lines) and six TOMAS cases with the highest (worst) NME statistic (solid dotted lines). For comparison, the observed initial moments are also plotted for each moment (dotted black lines).

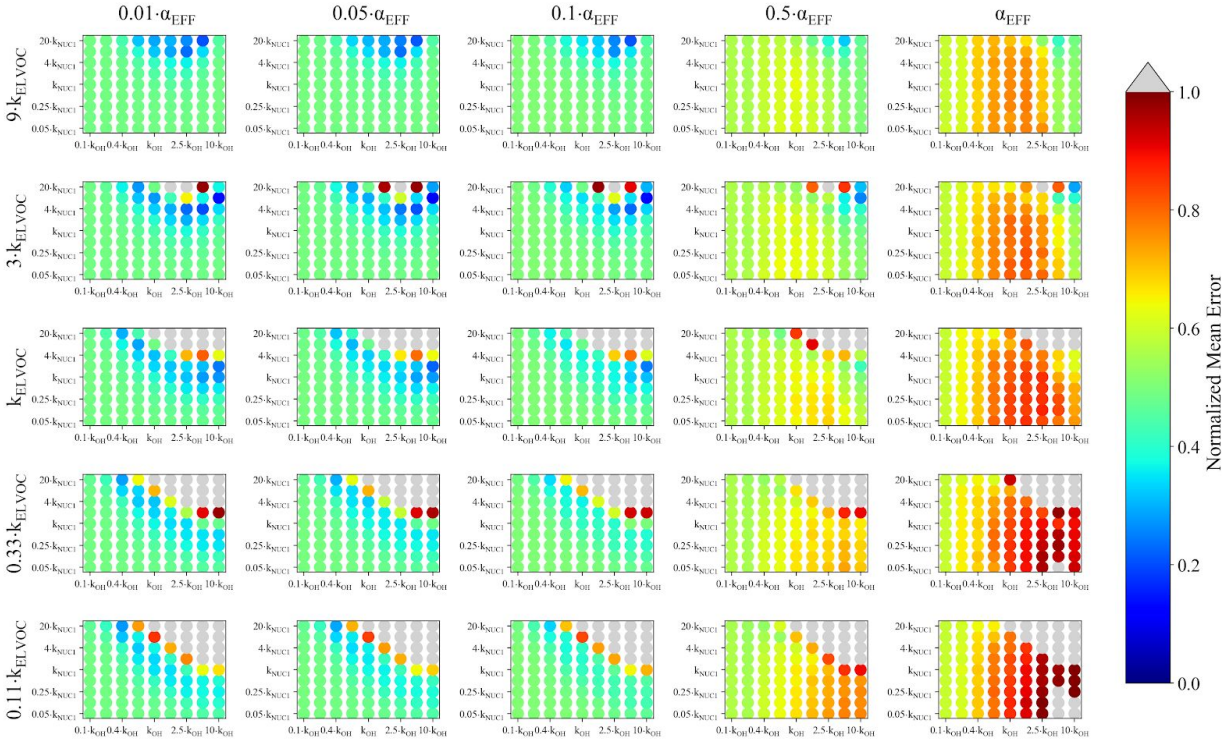

Figure S3. Representation of the parameter space for a 0.090 eq. day aging exposure from BEACHON-RoMBAS for the NUC1 nucleation scheme and base value of the reactive uptake coefficient of 0.6. The effective accommodation coefficient increases across each row of panels; the rate constant of gas-phase fragmentation increases up each column of panels. Within each panel, the rate constant of gas-phase reactions with OH increases along the x-axis and the rate constant for nucleation increases along the y-axis. The color bar indicates the normalized mean error (NME) value for each simulation, with the lowest values indicating the least error between model and measurement. Grey regions indicate regions within the parameter space whose NME value is greater than 1.

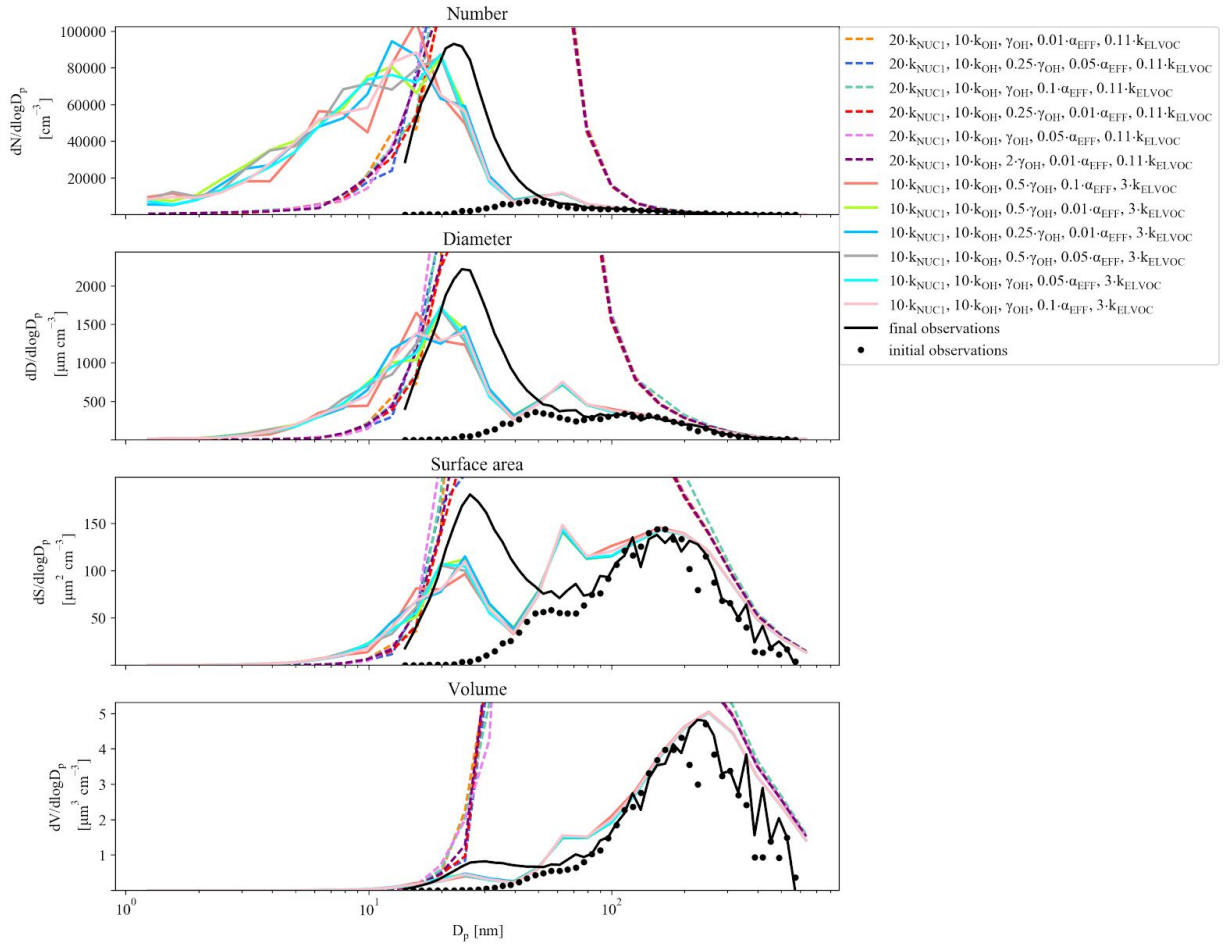

Figure S4. Example of best (solid lines) and worst (dashed lines) fit size distributions compared to the observed (black line) final OFR size distribution for a 0.090 eq days aging case from BEACHON-RoMBAS for the NUC1 nucleation scheme. The fits are determined using the mean error of moments method (see methods); each panel represents a separate moment. The top panel represents the number distribution; the second panel represents the diameter distribution; the third panel represents the surface area distribution; and the final (bottom) distribution represents the volume distribution.

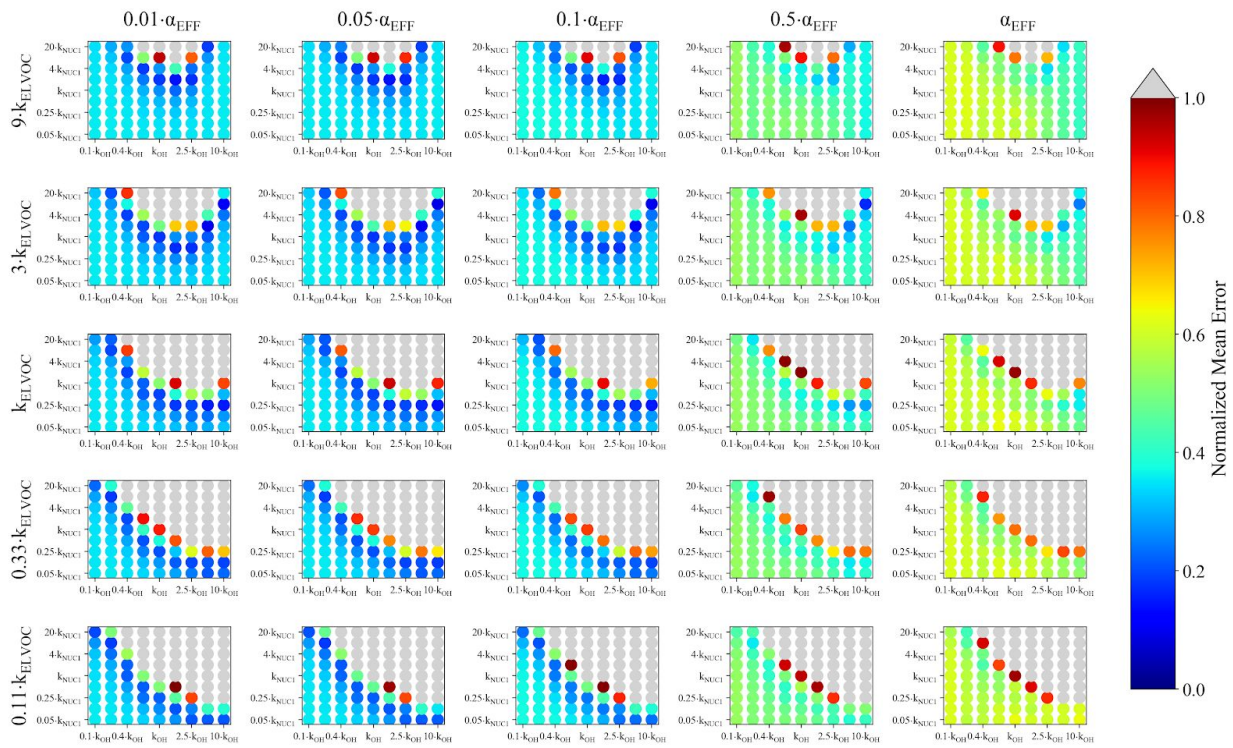

Figure S5. Representation of the parameter space for a 0.098 eq. day aging exposure from BEACHON-RoMBAS for the NUC1 nucleation scheme and base value of the reactive uptake coefficient of 0.6. The effective accommodation coefficient increases across each row of panels; the rate constant of gas-phase fragmentation increases up each column of panels. Within each panel, the rate constant of gas-phase reactions with OH increases along the x-axis and the rate constant for nucleation increases along the y-axis. The color bar indicates the normalized mean error (NME) value for each simulation, with the lowest values indicating the least error between model and measurement. Grey regions indicate regions within the parameter space whose NME value is greater than 1.

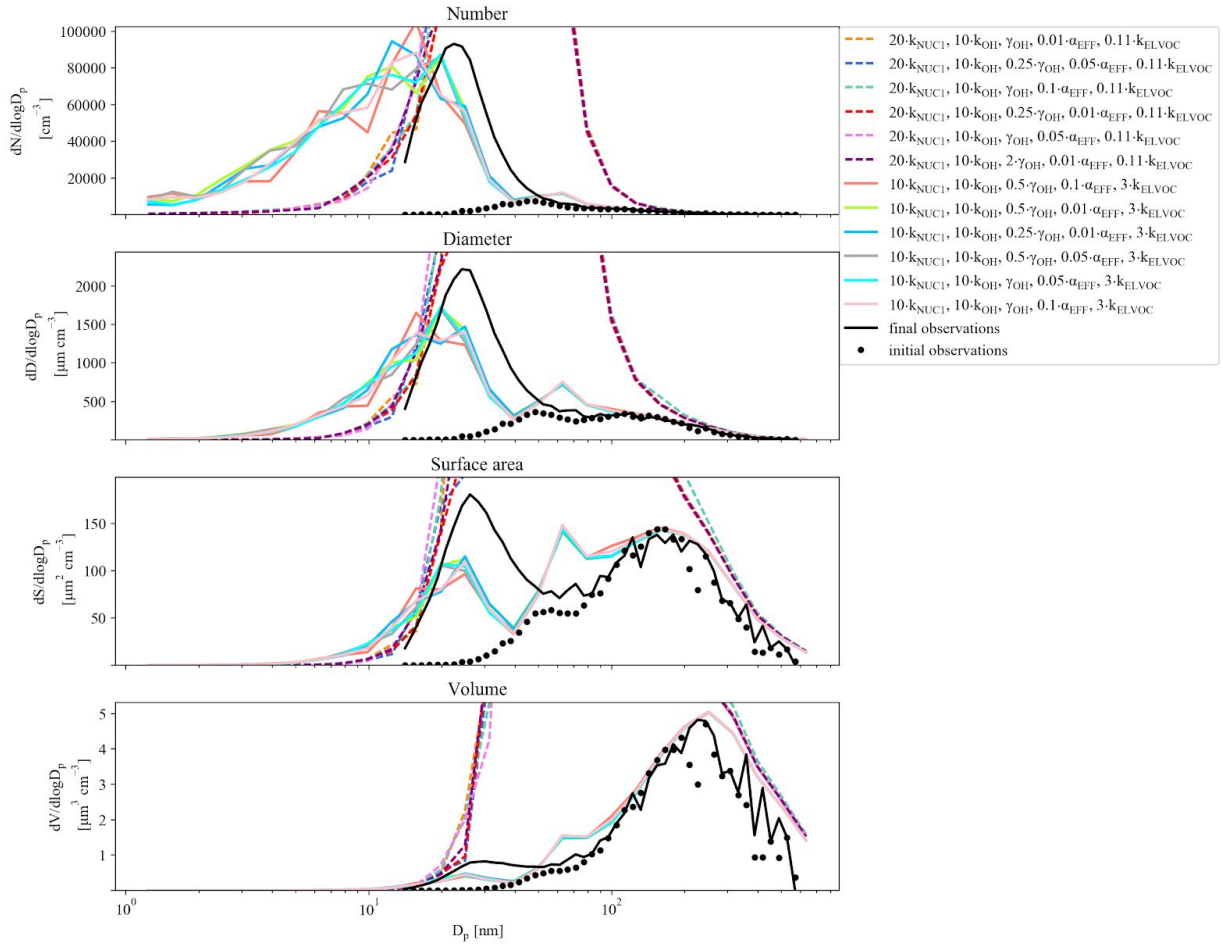

Figure S6. Example of best (solid lines) and worst (dashed lines) fit size distributions compared to the observed (black line) final OFR size distribution for a 0.098 eq days aging case from BEACHON-RoMBAS for the NUC1 nucleation scheme. The fits are determined using the mean error of moments method (see methods); each panel represents a separate moment. The top panel represents the number distribution; the second panel represents the diameter distribution; the third panel represents the surface area distribution; and the final (bottom) distribution represents the volume distribution.

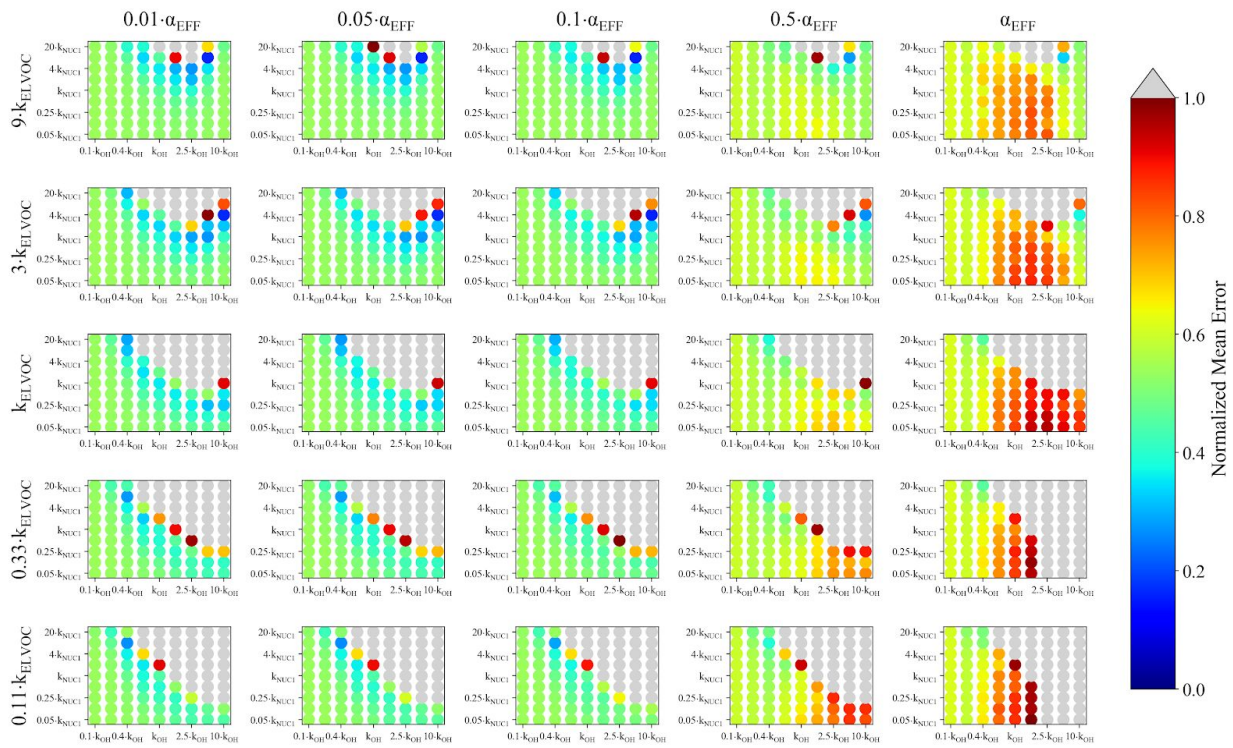

Figure S7. Representation of the parameter space for a 0.16 eq. day aging exposure from BEACHON-RoMBAS for the NUC1 nucleation scheme and base value of the reactive uptake coefficient of 0.6. The effective accommodation coefficient increases across each row of panels; the rate constant of gas-phase fragmentation increases up each column of panels. Within each panel, the rate constant of gas-phase reactions with OH increases along the x-axis and the rate constant for nucleation increases along the y-axis. The color bar indicates the normalized mean error (NME) value for each simulation, with the lowest values indicating the least error between model and measurement. Grey regions indicate regions within the parameter space whose NME value is greater than 1.

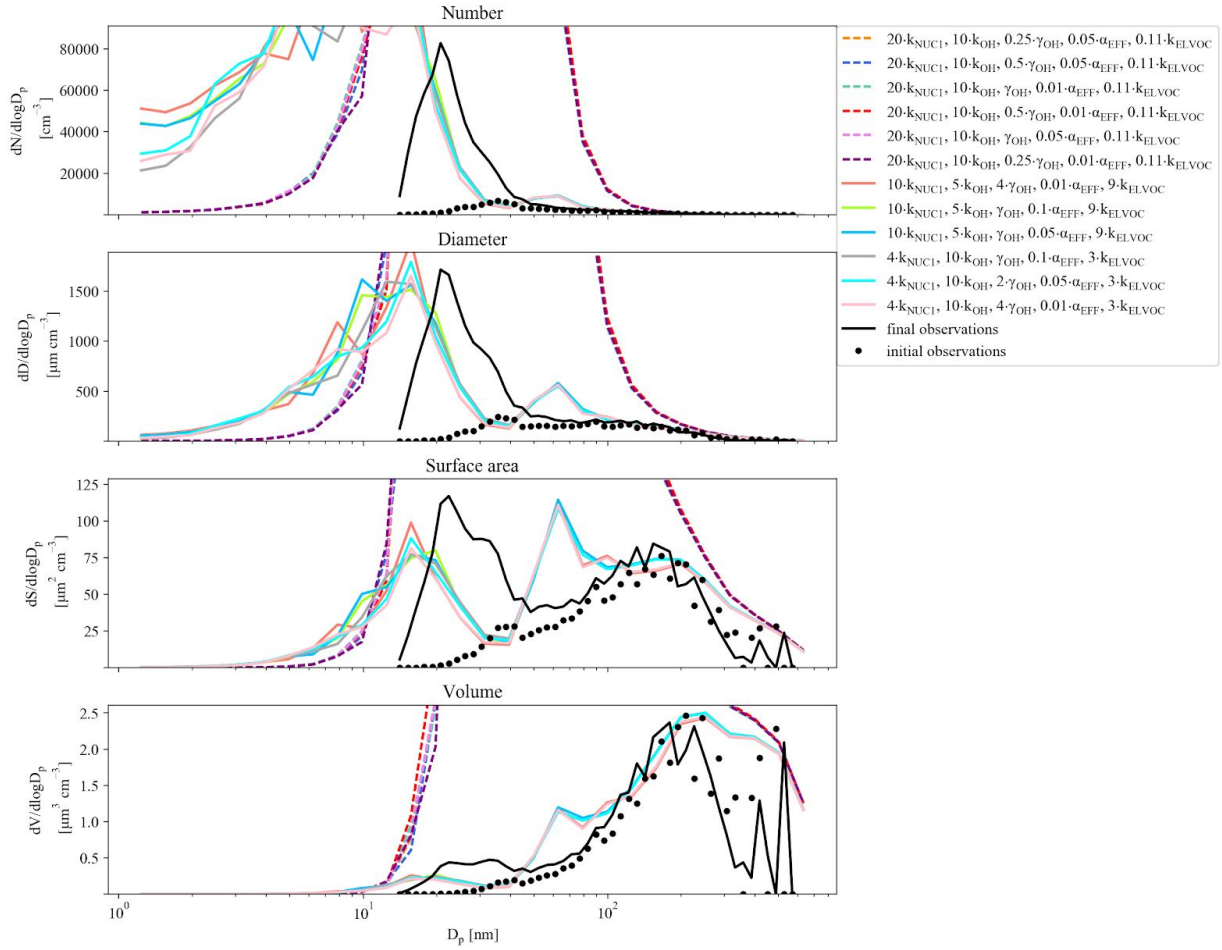

Figure S8. Example of best (solid lines) and worst (dashed lines) fit size distributions compared to the observed (black line) final OFR size distribution for a 0.16 eq days aging case from BEACHON-RoMBAS for the NUC1 nucleation scheme. The fits are determined using the mean error of moments method (see methods); each panel represents a separate moment. The top panel represents the number distribution; the second panel represents the diameter distribution; the third panel represents the surface area distribution; and the final (bottom) distribution represents the volume distribution.

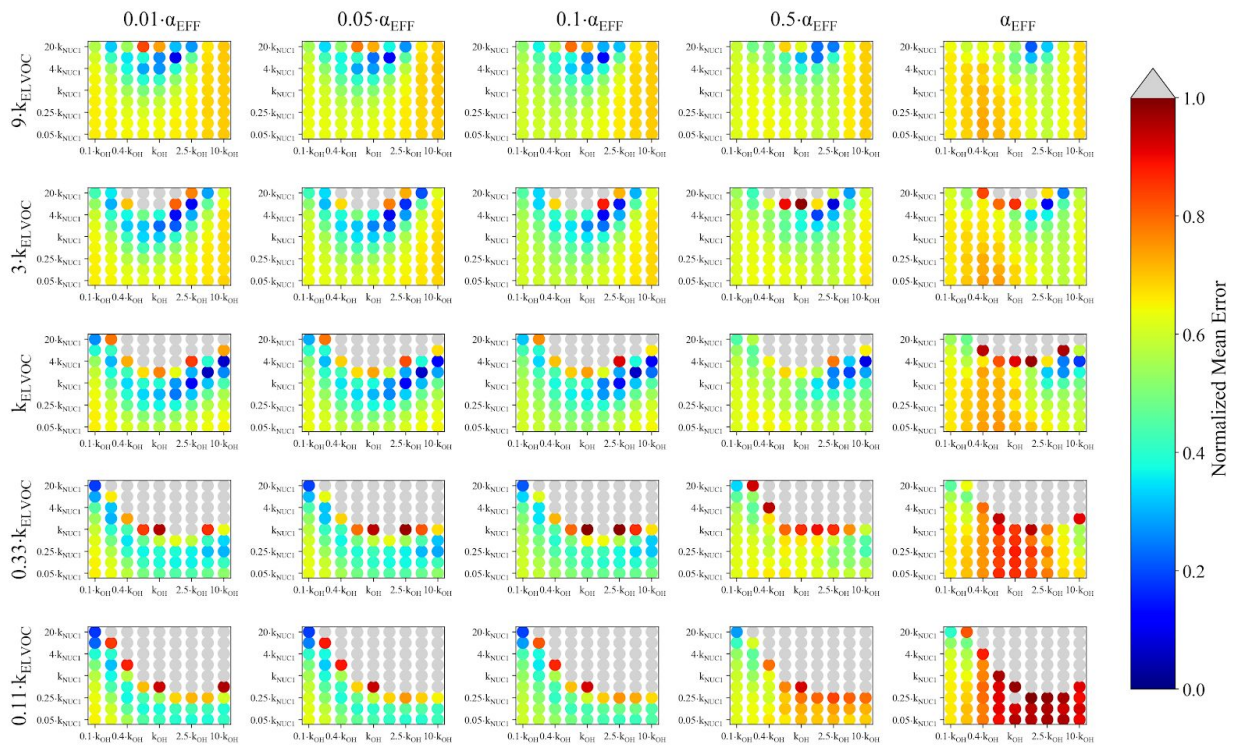

Figure S9. Representation of the parameter space for a 0.23 eq. day aging exposure from BEACHON-RoMBAS for the NUC1 nucleation scheme and base value of the reactive uptake coefficient of 0.6. The effective accommodation coefficient increases across each row of panels; the rate constant of gas-phase fragmentation increases up each column of panels. Within each panel, the rate constant of gas-phase reactions with OH increases along the x-axis and the rate constant for nucleation increases along the y-axis. The color bar indicates the normalized mean error (NME) value for each simulation, with the lowest values indicating the least error between model and measurement. Grey regions indicate regions within the parameter space whose NME value is greater than 1.

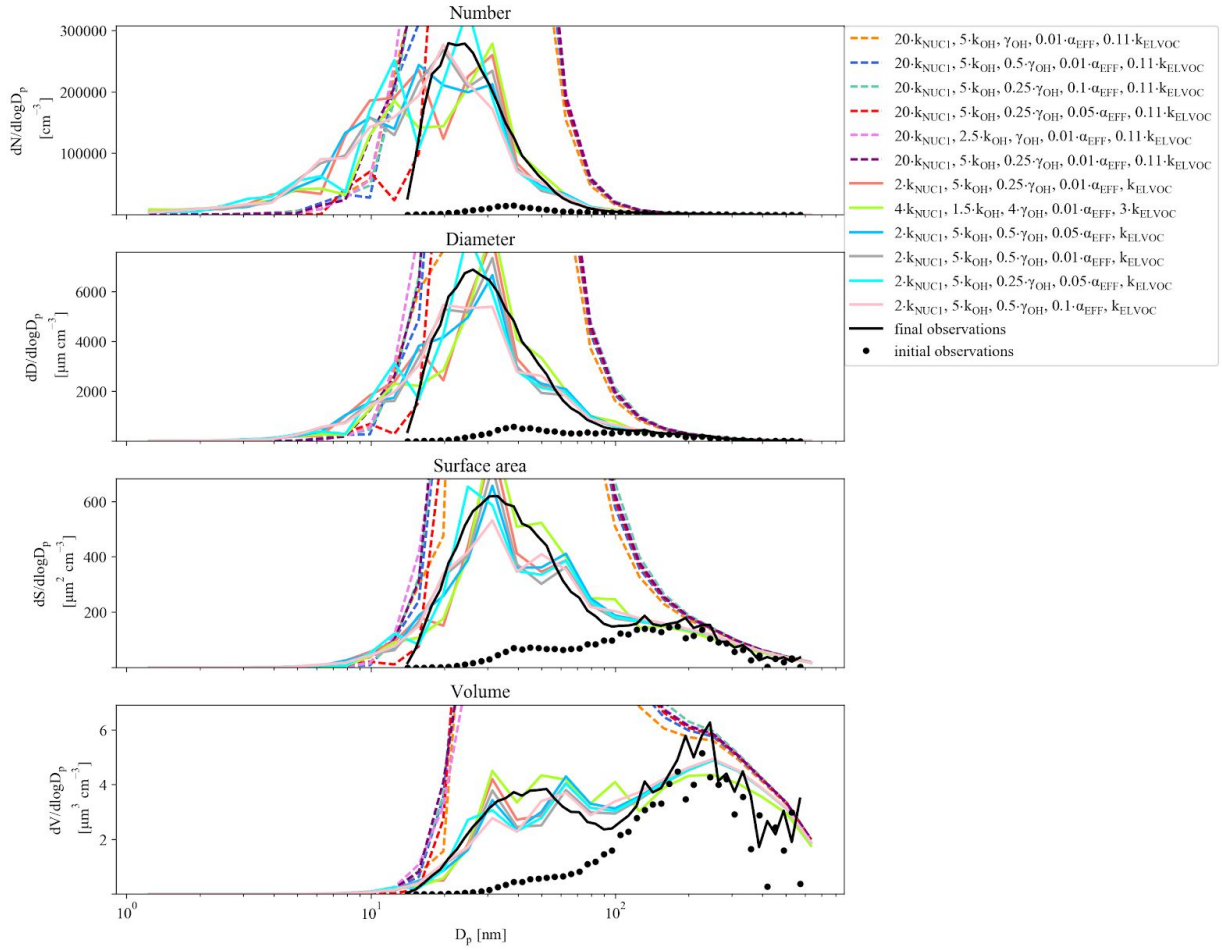

Figure S10. Example of best (solid lines) and worst (dashed lines) fit size distributions compared to the observed (black line) final OFR size distribution for a 0.23 eq days aging case from BEACHON-RoMBAS for the NUC1 nucleation scheme. The fits are determined using the mean error of moments method (see methods); each panel represents a separate moment. The top panel represents the number distribution; the second panel represents the diameter distribution; the third panel represents the surface area distribution; and the final (bottom) distribution represents the volume distribution.

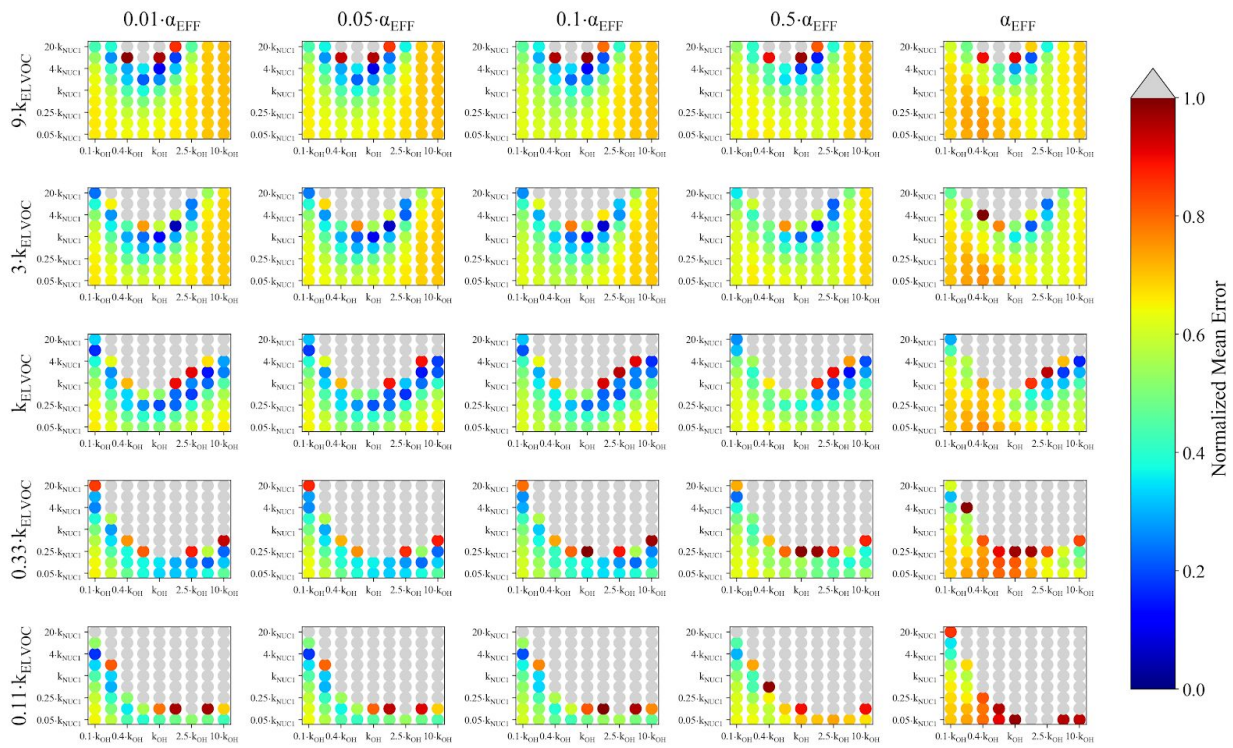

Figure S11. Representation of the parameter space for a 0.27 eq. day aging exposure from BEACHON-RoMBAS for the NUC1 nucleation scheme and base value of the reactive uptake coefficient of 0.6. The effective accommodation coefficient increases across each row of panels; the rate constant of gas-phase fragmentation increases up each column of panels. Within each panel, the rate constant of gas-phase reactions with OH increases along the x-axis and the rate constant for nucleation increases along the y-axis. The color bar indicates the normalized mean error (NME) value for each simulation, with the lowest values indicating the least error between model and measurement. Grey regions indicate regions within the parameter space whose NME value is greater than 1.

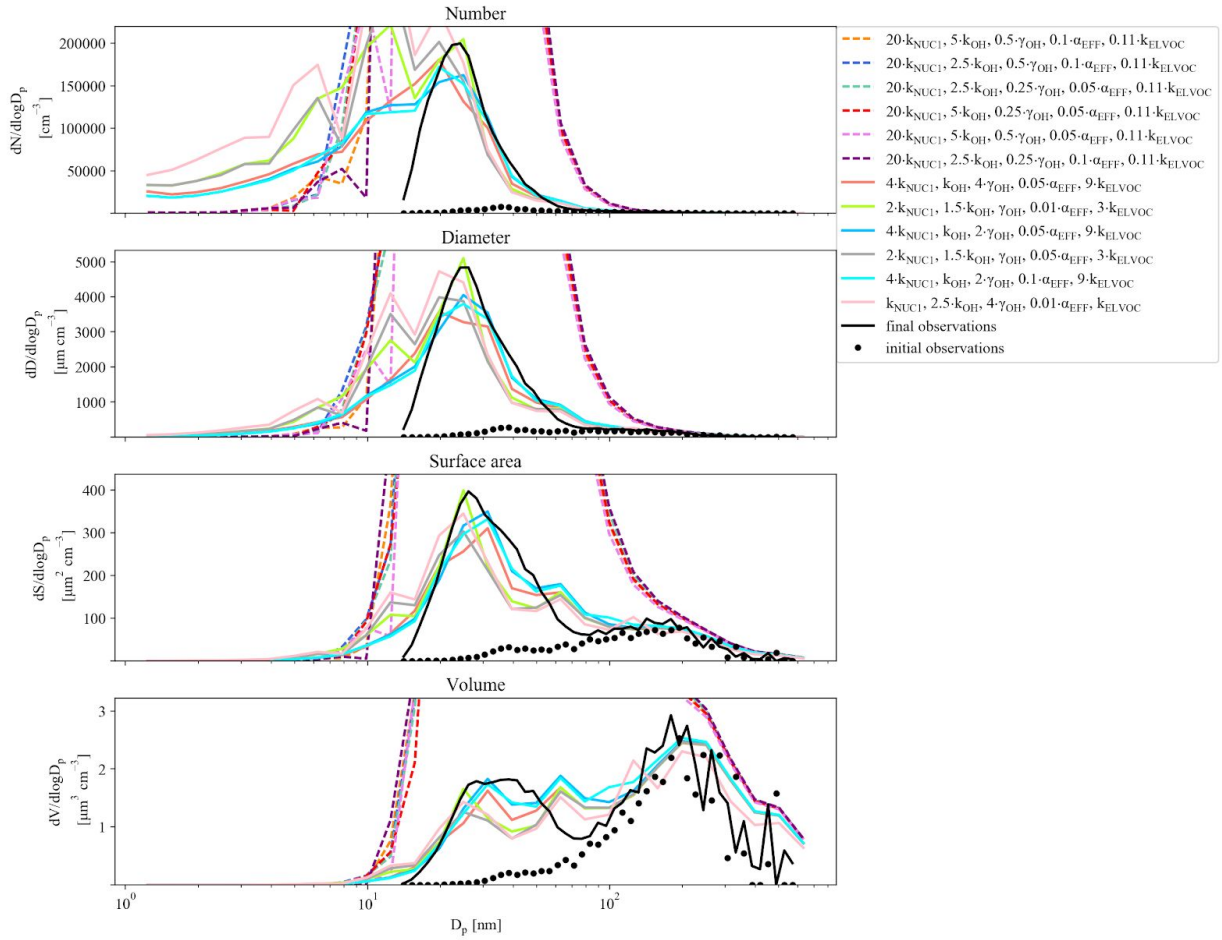

Figure S12. Example of best (solid lines) and worst (dashed lines) fit size distributions compared to the observed (black line) final OFR size distribution for a 0.27 eq days aging case from BEACHON-RoMBAS for the NUC1 nucleation scheme. The fits are determined using the mean error of moments method (see methods); each panel represents a separate moment. The top panel represents the number distribution; the second panel represents the diameter distribution; the third panel represents the surface area distribution; and the final (bottom) distribution represents the volume distribution.

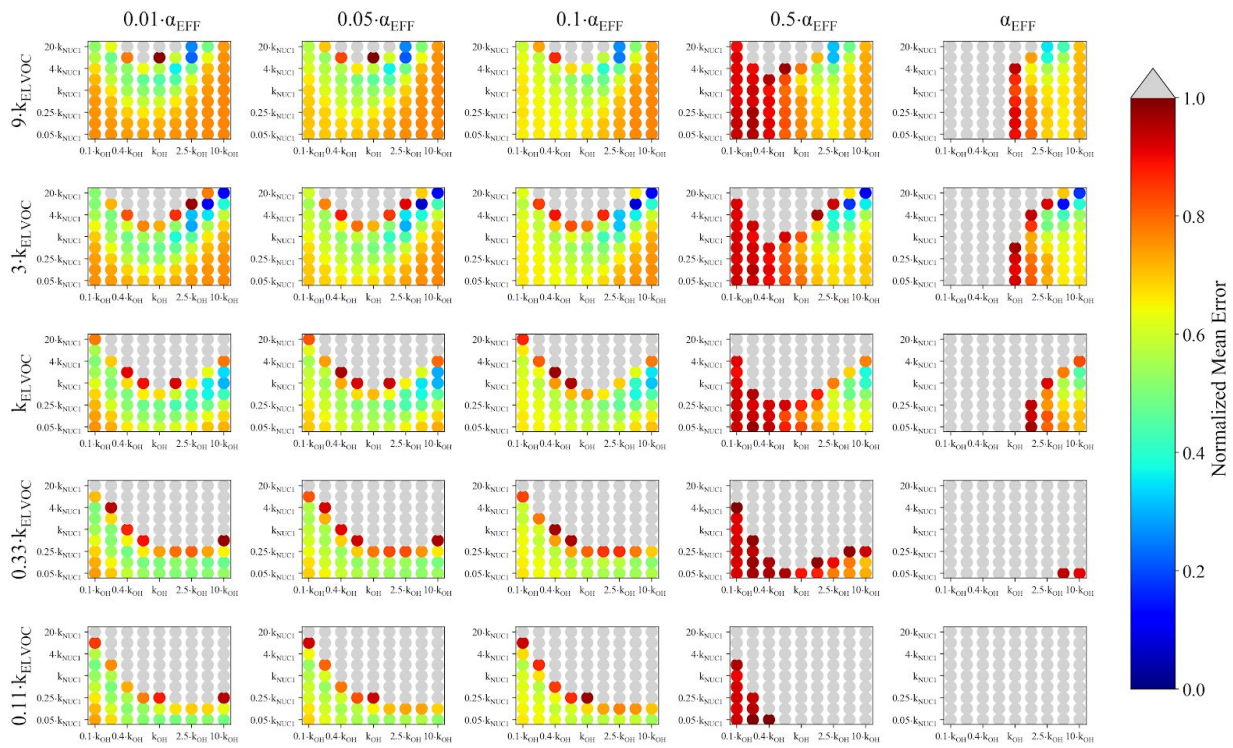

Figure S13. Representation of the parameter space for a 0.77 eq. day aging exposure from BEACHON-RoMBAS for the NUC1 nucleation scheme and base value of the reactive uptake coefficient of 0.6. The effective accommodation coefficient increases across each row of panels; the rate constant of gas-phase fragmentation increases up each column of panels. Within each panel, the rate constant of gas-phase reactions with OH increases along the x-axis and the rate constant for nucleation increases along the y-axis. The color bar indicates the normalized mean error (NME) value for each simulation, with the lowest values indicating the least error between model and measurement. Grey regions indicate regions within the parameter space whose NME value is greater than 1.

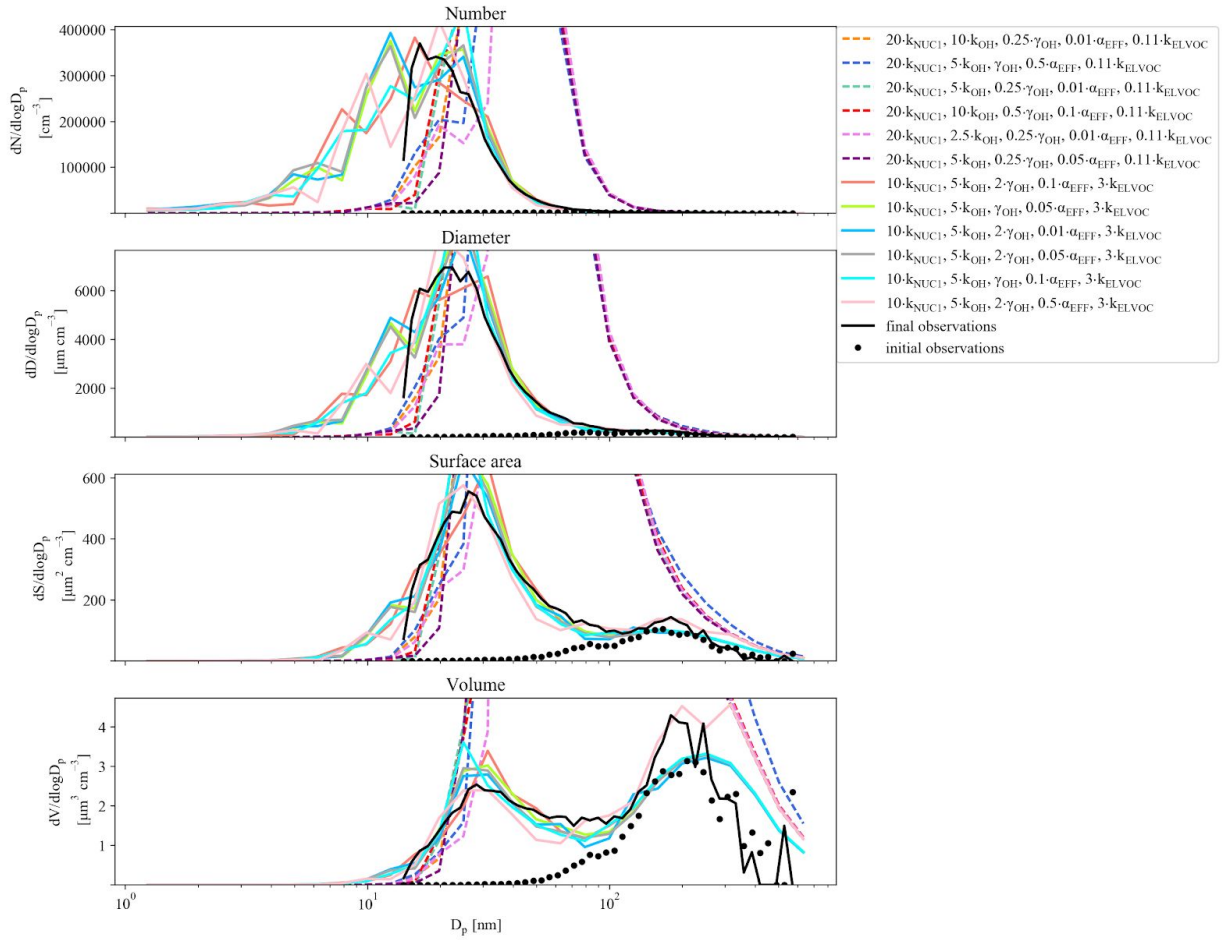

Figure S14. Example of best (solid lines) and worst (dashed lines) fit size distributions compared to the observed (black line) final OFR size distribution for a 0.77 eq days aging case from BEACHON-RoMBAS for the NUC1 nucleation scheme. The fits are determined using the mean error of moments method (see methods); each panel represents a separate moment. The top panel represents the number distribution; the second panel represents the diameter distribution; the third panel represents the surface area distribution; and the final (bottom) distribution represents the volume distribution.

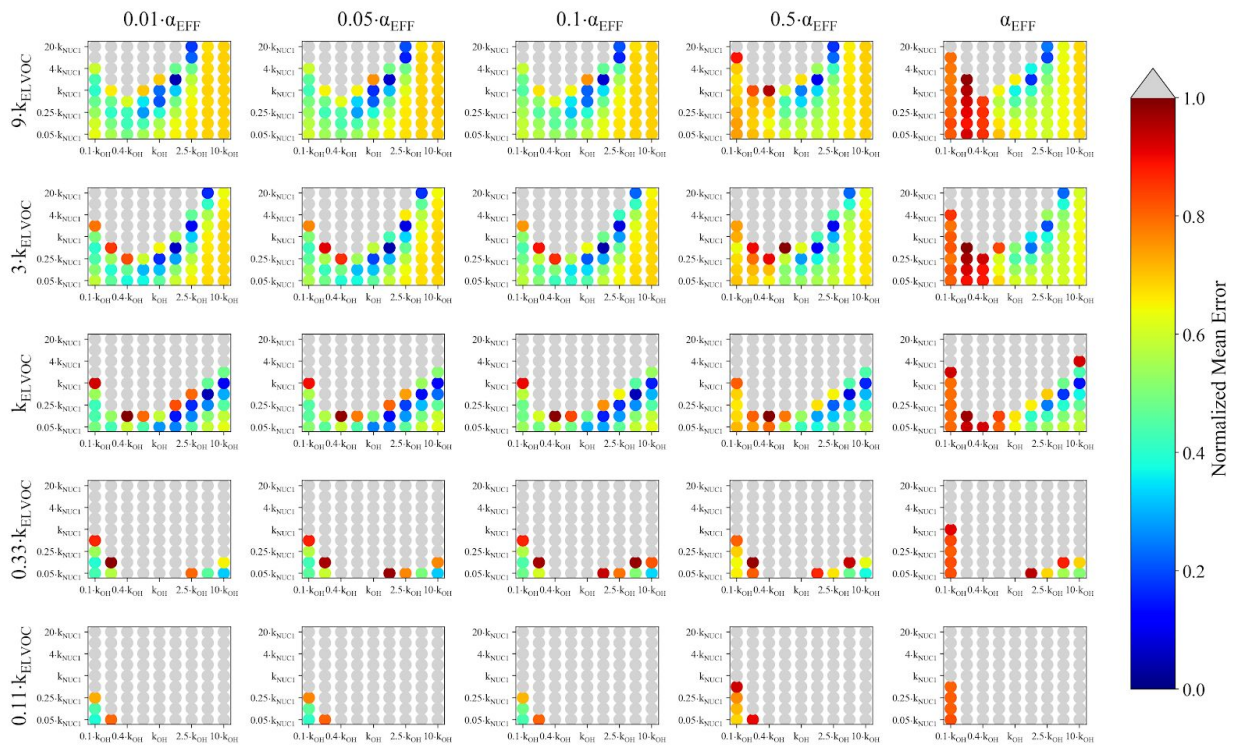

Figure S15. Representation of the parameter space for a 0.82 eq. day aging exposure from BEACHON-RoMBAS for the NUC1 nucleation scheme and base value of the reactive uptake coefficient of 0.6. The effective accommodation coefficient increases across each row of panels; the rate constant of gas-phase fragmentation increases up each column of panels. Within each panel, the rate constant of gas-phase reactions with OH increases along the x-axis and the rate constant for nucleation increases along the y-axis. The color bar indicates the normalized mean error (NME) value for each simulation, with the lowest values indicating the least error between model and measurement. Grey regions indicate regions within the parameter space whose NME value is greater than 1.

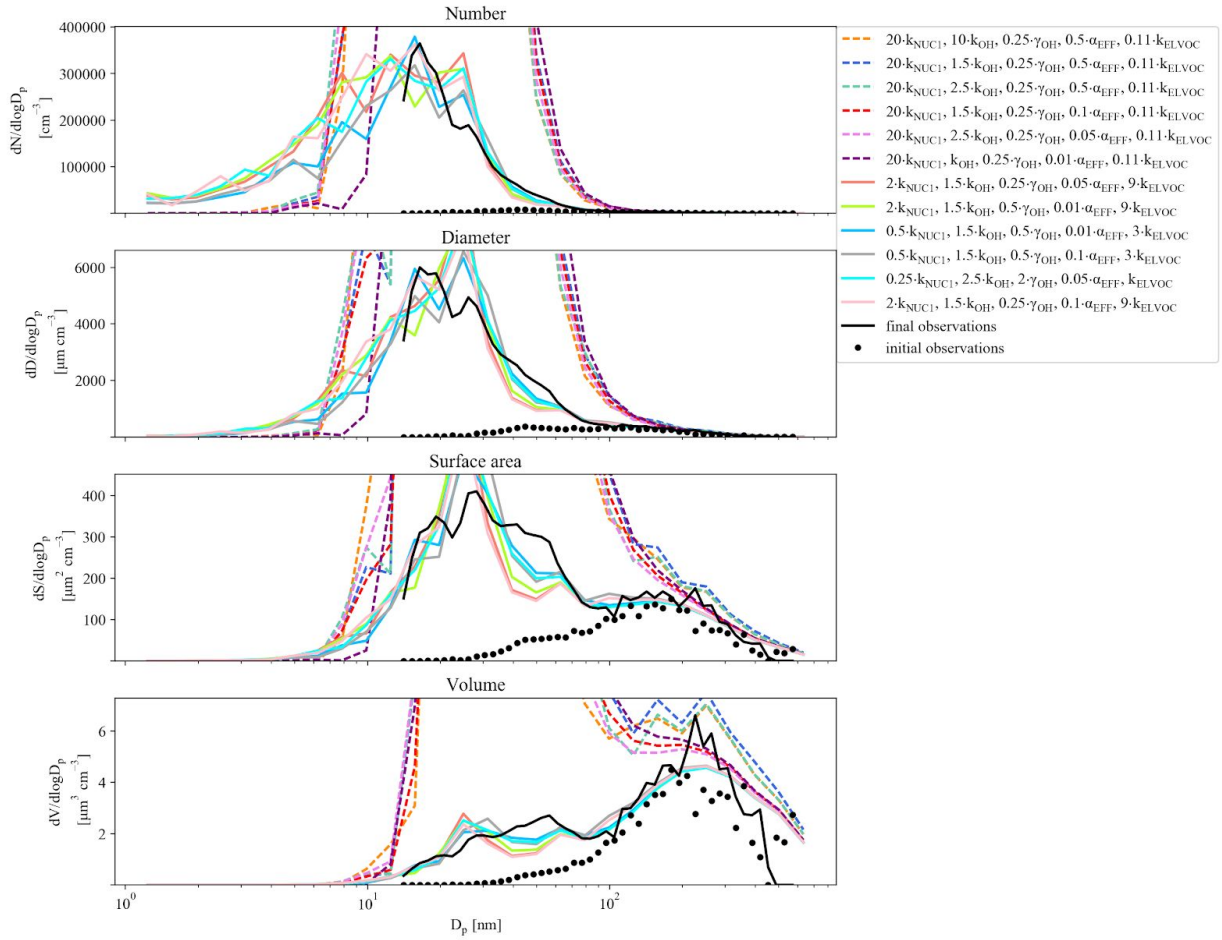

Figure S16. Example of best (solid lines) and worst (dashed lines) fit size distributions compared to the observed (black line) final OFR size distribution for a 0.82 eq days aging case from BEACHON-RoMBAS for the NUC1 nucleation scheme. The fits are determined using the mean error of moments method (see methods); each panel represents a separate moment. The top panel represents the number distribution; the second panel represents the diameter distribution; the third panel represents the surface area distribution; and the final (bottom) distribution represents the volume distribution.

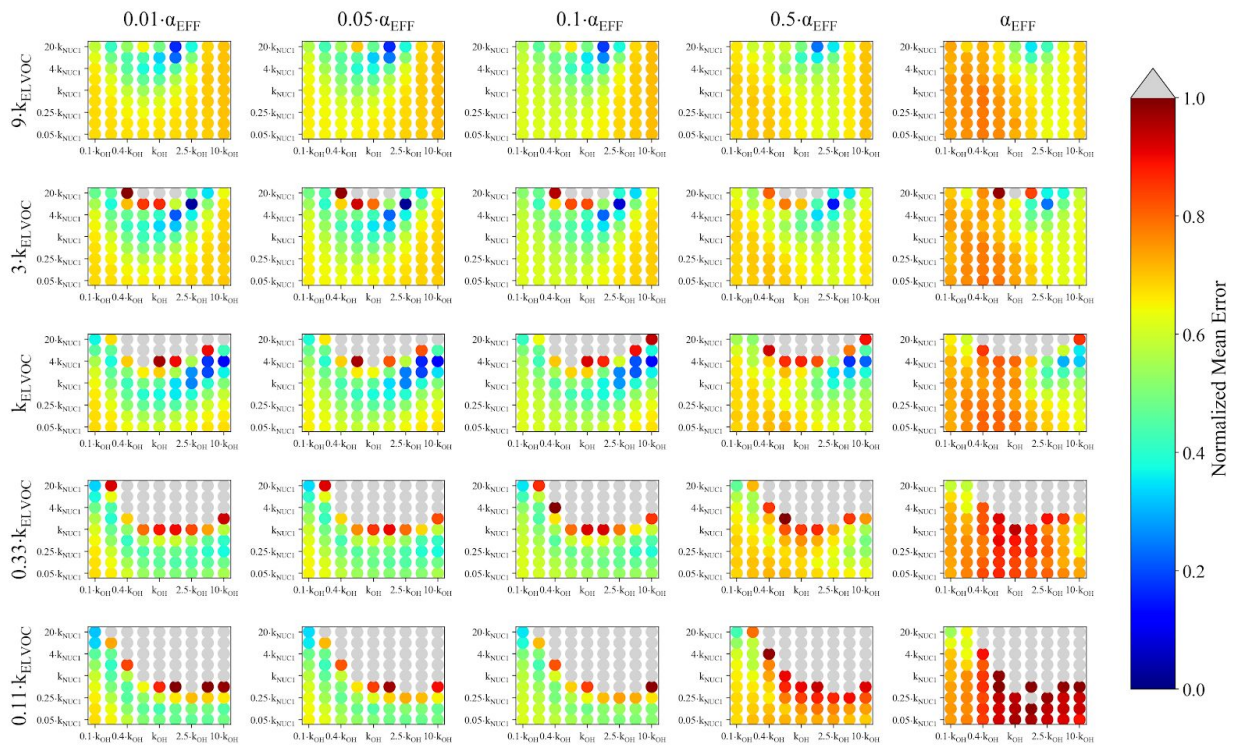

Figure S17. Representation of the parameter space for a 0.91 eq. day aging exposure from BEACHON-RoMBAS for the NUC1 nucleation scheme and base value of the reactive uptake coefficient of 0.6. The effective accommodation coefficient increases across each row of panels; the rate constant of gas-phase fragmentation increases up each column of panels. Within each panel, the rate constant of gas-phase reactions with OH increases along the x-axis and the rate constant for nucleation increases along the y-axis. The color bar indicates the normalized mean error (NME) value for each simulation, with the lowest values indicating the least error between model and measurement. Grey regions indicate regions within the parameter space whose NME value is greater than 1.

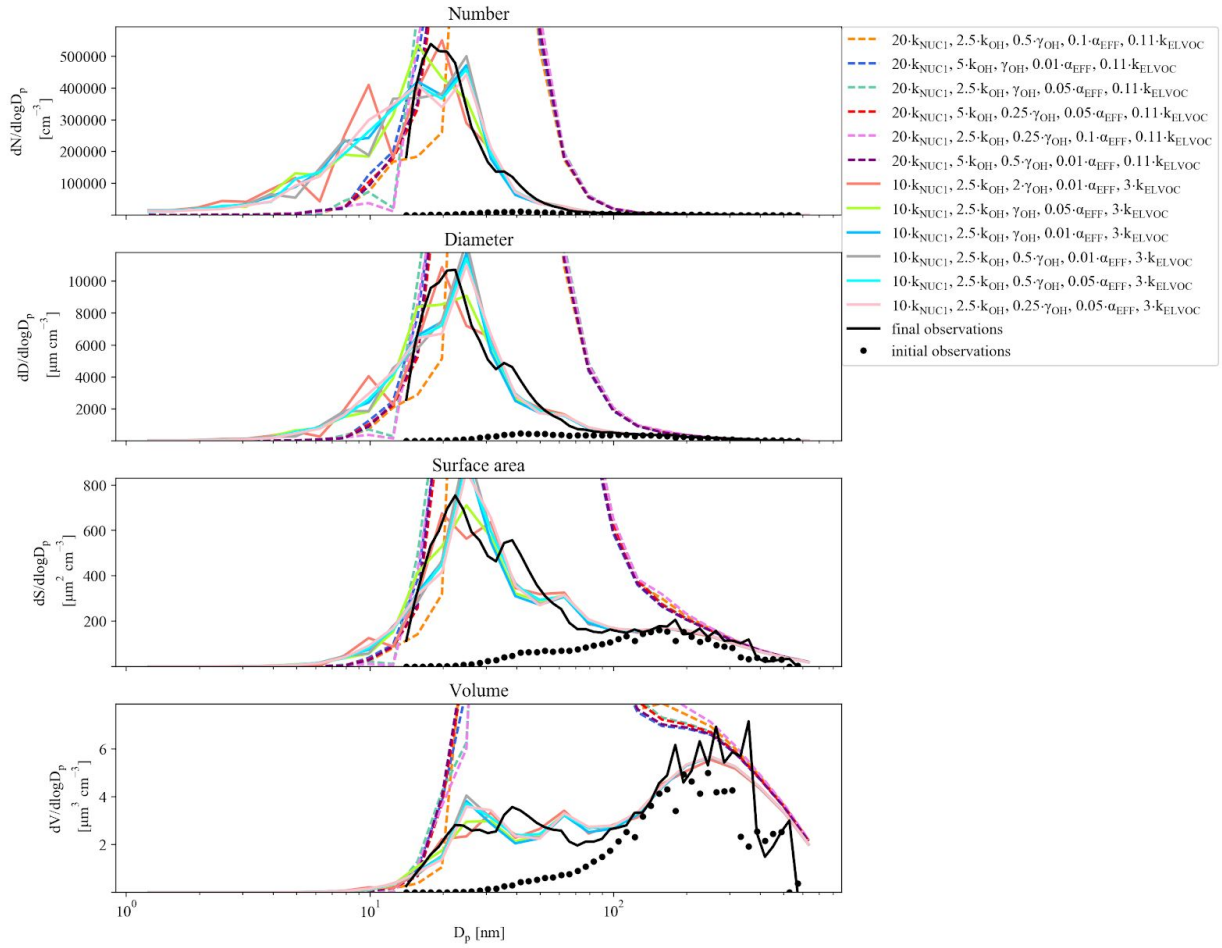

Figure S18. Example of best (solid lines) and worst (dashed lines) fit size distributions compared to the observed (black line) final OFR size distribution for a 0.91 eq days aging case from BEACHON-RoMBAS for the NUC1 nucleation scheme. The fits are determined using the mean error of moments method (see methods); each panel represents a separate moment. The top panel represents the number distribution; the second panel represents the diameter distribution; the third panel represents the surface area distribution; and the final (bottom) distribution represents the volume distribution.

S3. Sensitivity of the model to the NUC2 nucleation scheme for BEACHON-RoMBAS

Figures S19 gives the average NME values across the 0.09-0.9 day eq. aging exposures from BEACHON-RoMBAS examined in this study for the parameter space that lies within (Table 3) the NUC2 nucleation scheme and base value of the reactive uptake coefficient. This figure is qualitatively similar to Fig. 5, which shows the same parameter space except for the NUC1 nucleation scheme.

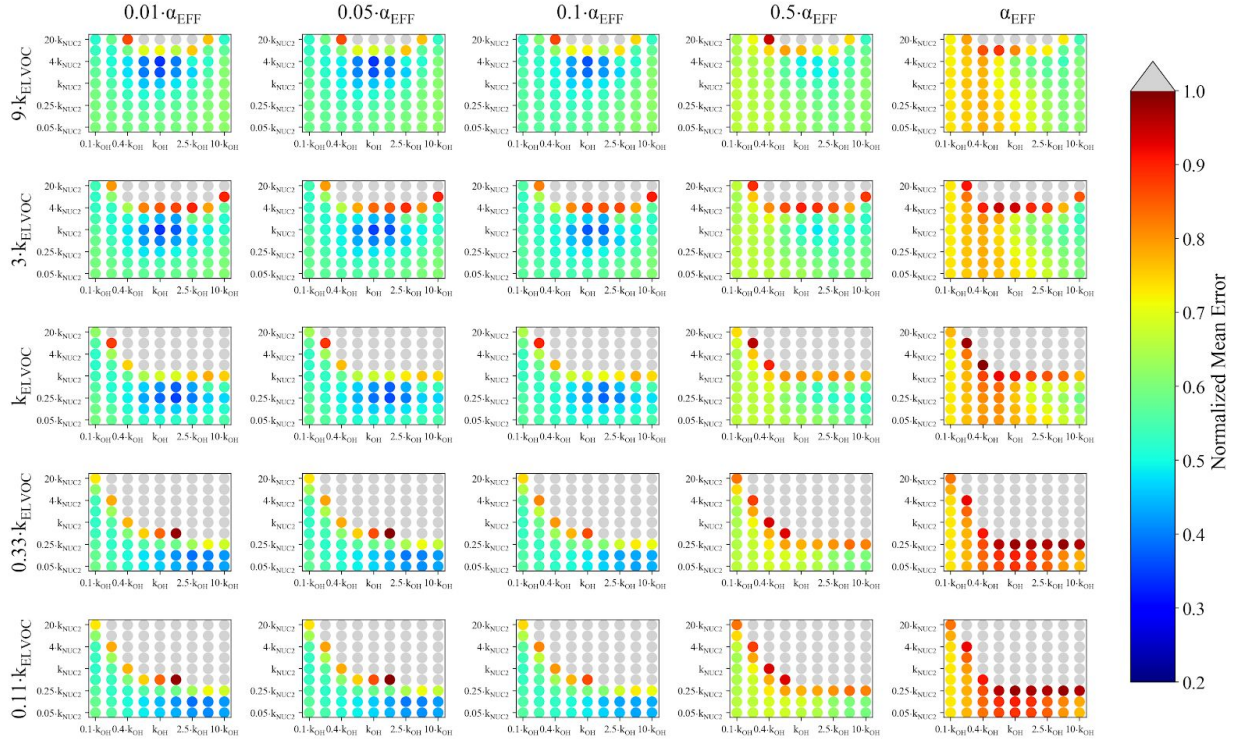

Figure S19. Representation of the parameter space for the average across the 0.09-0.9 day eq. aging exposures from BEACHON-RoMBAS examined in this study for the NUC2 nucleation scheme and base value of the reactive uptake coefficient of 0.6. The effective accommodation coefficient increases across each row of panels; the rate constant of gas-phase fragmentation increases up each column of panels. Within each panel, the rate constant of gas-phase reactions with OH increases along the x-axis and the rate constant for nucleation increases along the y-axis. The color bar indicates the normalized mean error (NME) value for each simulation, with the lowest values indicating the least error between model and measurement. Grey regions indicate regions within the parameter space whose NME value is greater than 1. No averaged case had a NME value less than 0.2 for the cases shown here.

S4. Sensitivity of the model to the heterogeneous chemistry parameter for BEACHON-RoMBAS

In order to determine the model sensitivity to the reactive uptake coefficient, γ_{OH}, we replot the results of Fig. 4 in Fig. S20 to be a function of γ_{OH} (increasing across each column) for the base value of the gas-phase fragmentation rate constant.

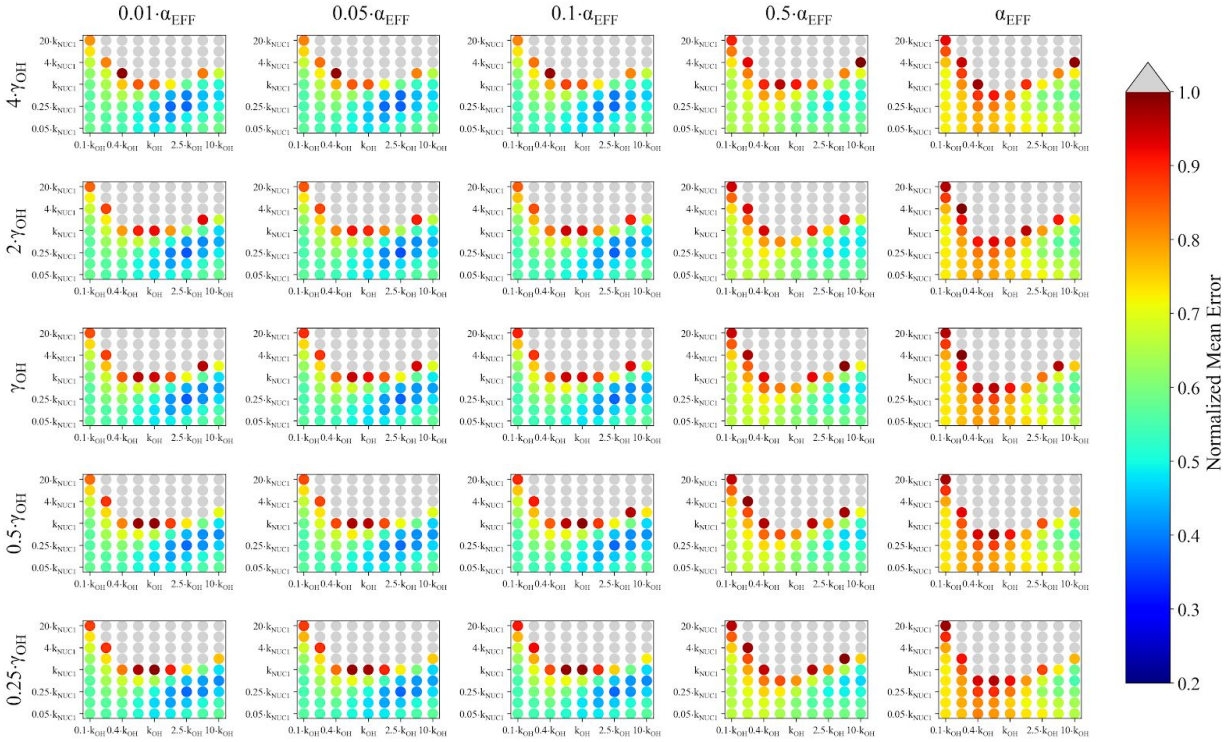

Figure S20. Representation of the parameter space for the average across the 0.09-0.9 day eq. aging exposures from BEACHON-RoMBAS examined in this study for the NUC1 nucleation scheme and base value of the gas-phase fragmentation rate constant (k_{ELVOC}). The effective accommodation increases across each row; the reactive uptake coefficient increases up each column of panels. Within each panel, the rate constant of gas-phase reactions with OH increases along the x-axis and the rate constant for nucleation increases along the y-axis. The color bar indicates the normalized mean error (NME) value for each simulation, with the lowest values indicating the least error between model and measurement. Grey regions indicate regions within the parameter space whose NME value is greater than 1. No averaged case had a NME value less than 0.2 for the cases shown here. This figure shows that for a fixed value of reactive uptake coefficient (each column), the NME values for each set of nucleation rate constants/gas-phase functionalization constants/effective accommodation coefficients do not show significant change.

S5. Sensitivity of the model to the k_{OH} formulation

All model runs in this paper have been performed using Eq. 1 in the main text for the gas-phase functionalization rate constant between organic vapors and OH:

$$k_{OH} = -5.7 \times 10^{-12} log10(C*) + 1.14 \times 10^{-10} \quad \text{(S1)}$$

This equation is from Jathar et al. (2014); however, the equation should instead be

$$k_{OH} = -5.7 \times 10^{-12} ln10(C*) + 1.14 \times 10^{-10} \quad \text{(S2)}$$

(S. Jathar, personal communication). Table S1 provides the k_{OH} values obtained from Eqs. S1 and S2. Figure S21 is a direct comparison to Fig. 4 of the main text, showing the results of the parameter space for the average across the 0.09-0.9 day eq. aging exposures from BEACHON-RoMBAS examined in this study, using the NUC1 nucleation scheme and base value of the reactive uptake coefficient of 0.6, and the k_{OH} formulation of Eq. S2, keeping all other parameter values identical to the values listed in Table 3. (We still test the same multipliers on k_{OH} listed in Table 3). Figure S22 provides the same figure as Fig. S21, but with the nucleation rate values (k_{NUCI}) each decreased by a factor of 10 from that of the values in Table 3. Although Fig. S22 well-matches the general shapes seen in Fig. 4 for each k_{ELVOC} and α_{EFF}, the normalized mean errors are larger in both Figs. S21 and S22 than in Fig. 4. Thus we conclude that for this study, using the k_{OH} values from Eq. S1 provide better fits and that parameterizations for rate constants for k_{OH} of air containing a mixture of ambient species require further investigation.

Table S1: k_{OH} values obtained from Eq. S1 (Eq. 1 of the main text) and Eq. S2 for each volatility bin used in this study.

C^* [μg m^{-3}]	k_{OH} from Eq. S1 [cm molec^{-1} s^{-1}]	k_{OH} from Eq. S2 [cm^3 molec^{-1} s^{-1}]
1×10^{-4}	1.36×10^{-10}	1.66×10^{-10}
1×10^{-2}	1.24×10^{-10}	1.40×10^{-10}
1×10^{0}	1.14×10^{-10}	1.14×10^{-10}
1×10^{2}	1.03×10^{-10}	8.78×10^{-11}
1×10^{4}	9.12×10^{-11}	6.15×10^{-11}
1×10^{6}	7.98×10^{-11}	3.53×10^{-11}

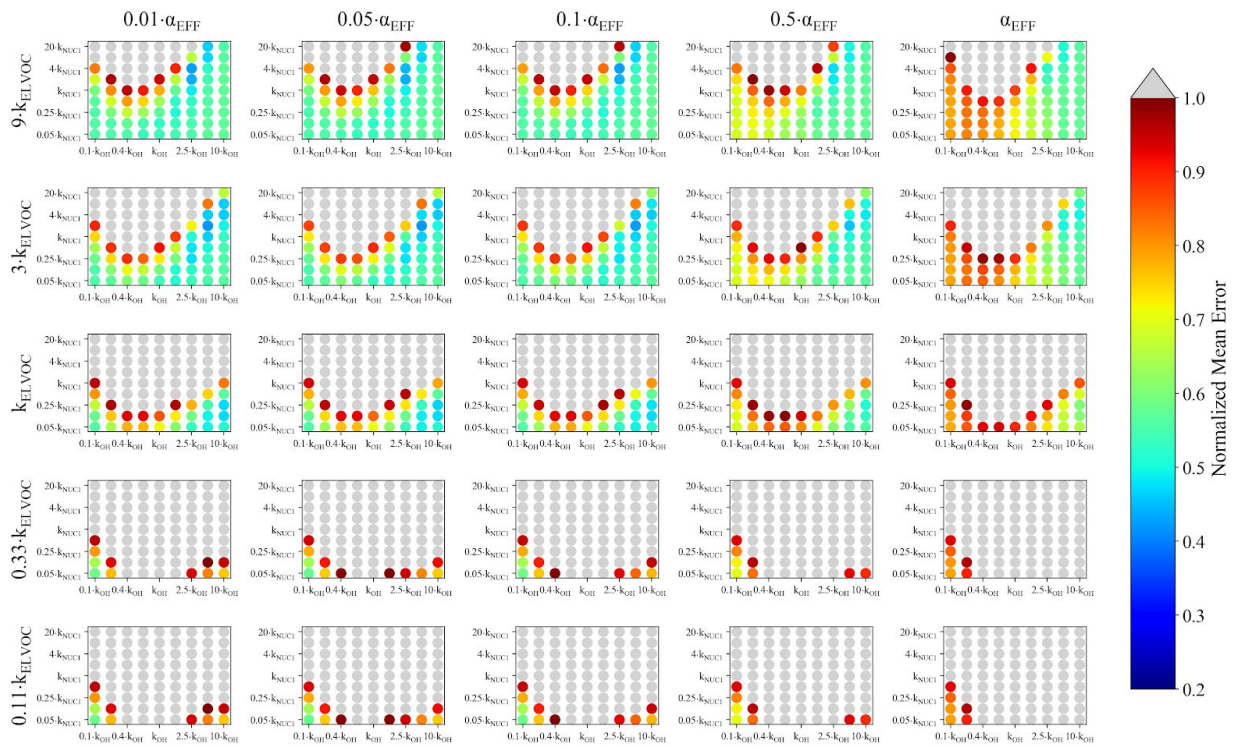

Figure S21. Representation of the parameter space for the average across the 0.09-0.9 day eq. aging exposures from BEACHON-RoMBAS examined in this study for the NUC1 nucleation scheme and base value of the reactive uptake coefficient of 0.6, using Eq. S2 for the values of k_{OH}. The effective accommodation coefficient increases across each row of panels; the rate constant of gas-phase fragmentation increases up each column of panels. Within each panel, the rate constant of gas-phase reactions with OH increases along the x-axis and the rate constant for nucleation increases along the y-axis. The color bar indicates the normalized mean error (NME) value for each simulation, with the lowest values indicating the least error between model and measurement. Grey regions indicate regions within the parameter space whose NME value is greater than 1. No averaged case had a NME value less than 0.2 for the cases shown here. This figure can be directly compared to Fig. 4 of the main text.

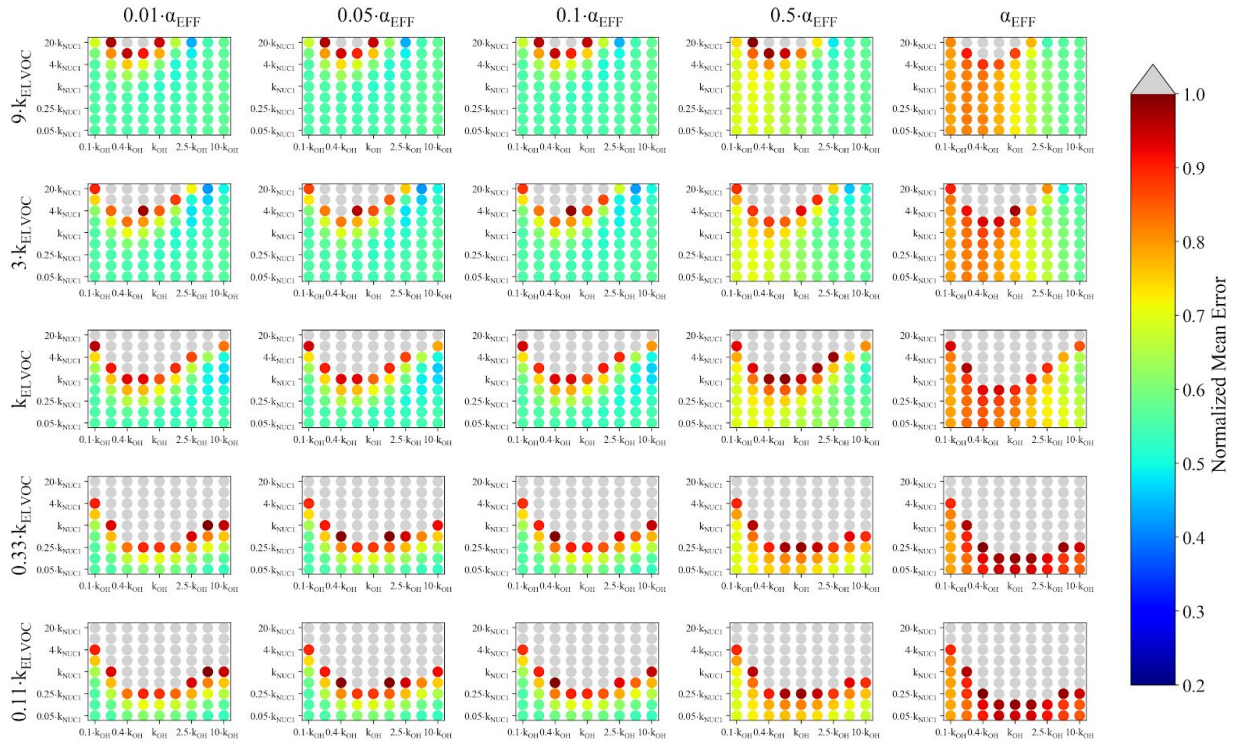

Figure S22. Representation of the parameter space for the average across the 0.09-0.9 day eq. aging exposures from BEACHON-RoMBAS examined in this study for the NUC1 nucleation scheme and base value of the reactive uptake coefficient of 0.6, using Eq. S2 for the values of k_{OH} and dividing each original k_{NUCl} value from Table 3 by a factor of 10. The effective accommodation coefficient increases across each row of panels; the rate constant of gas-phase fragmentation increases up each column of panels. Within each panel, the rate constant of gas-phase reactions with OH increases along the x-axis and the rate constant for nucleation increases along the y-axis. The color bar indicates the normalized mean error (NME) value for each simulation, with the lowest values indicating the least error between model and measurement. Grey regions indicate regions within the parameter space whose NME value is greater than 1. No averaged case had a NME value less than 0.2 for the cases shown here.

S6. GoAmazon sensitivity to S/IVOCs

To model the GoAmazon OFR distributions, we initially run TOMAS with the S/IVOC input concentration derived by using the campaign average ratio of MT:S/IVOCs from BEACHON-RoMBAS (Table 2), as S/IVOCs were not measured during the GoAmazon campaign. Figures S23 and S24 show that for this initial assumed S/IVOC concentration, we cannot replicate the observed growth (Fig. S24, black solid lines) and instead get poor NME values for all combinations of parameters (Fig. S23).

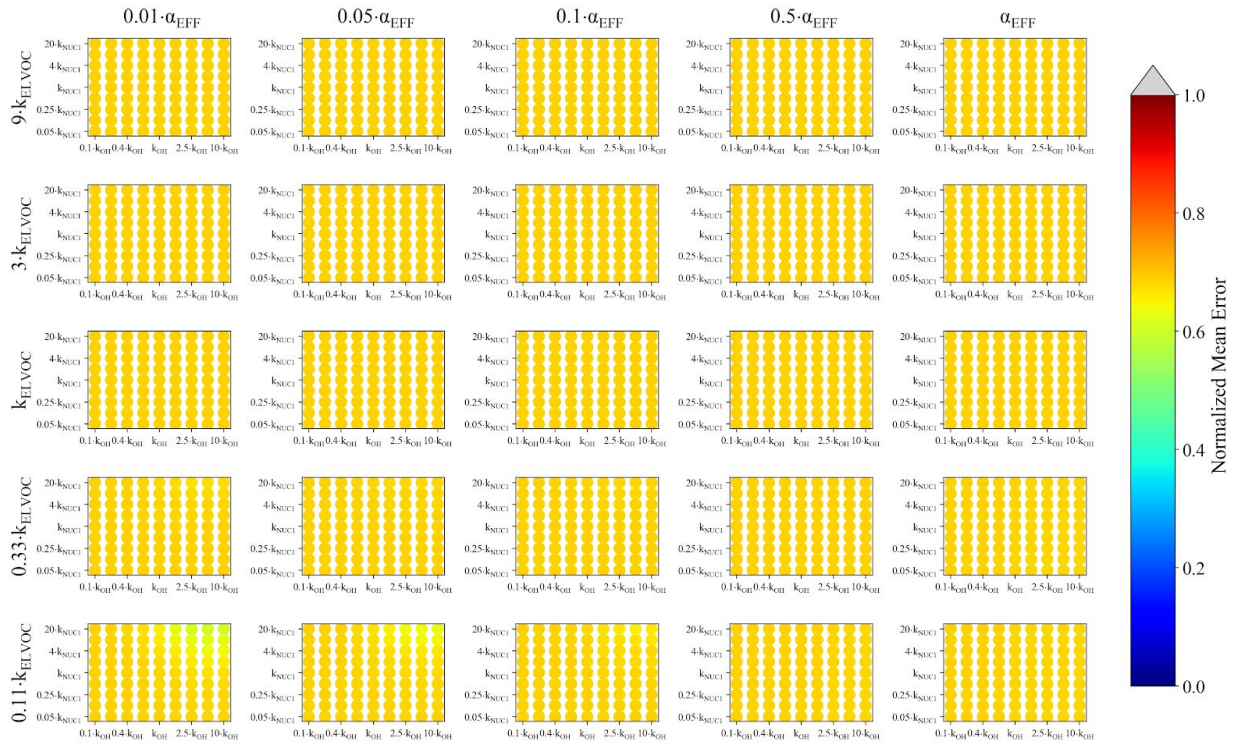

Figure S23. Representation of the parameter space for a 0.53 eq. day aging exposure from GoAmazon for the NUC1 nucleation scheme and base value of the reactive uptake coefficient of 0.6. The effective accommodation coefficient increases across each row of panels; the rate constant of gas-phase fragmentation increases up each column of panels. Within each panel, the rate constant of gas-phase reactions with OH increases along the x-axis and the rate constant for nucleation increases along the y-axis. The color bar indicates the normalized mean error (NME) value for each simulation, with the lowest values indicating the least error between model and measurement. Grey regions indicate regions within the parameter space whose NME value is greater than 1. In order to see enough growth in the Aitken mode, an increase of between 20-40 times the original S/IVOC input is required. See text and Figs. 6 and S23-S29 for more details.

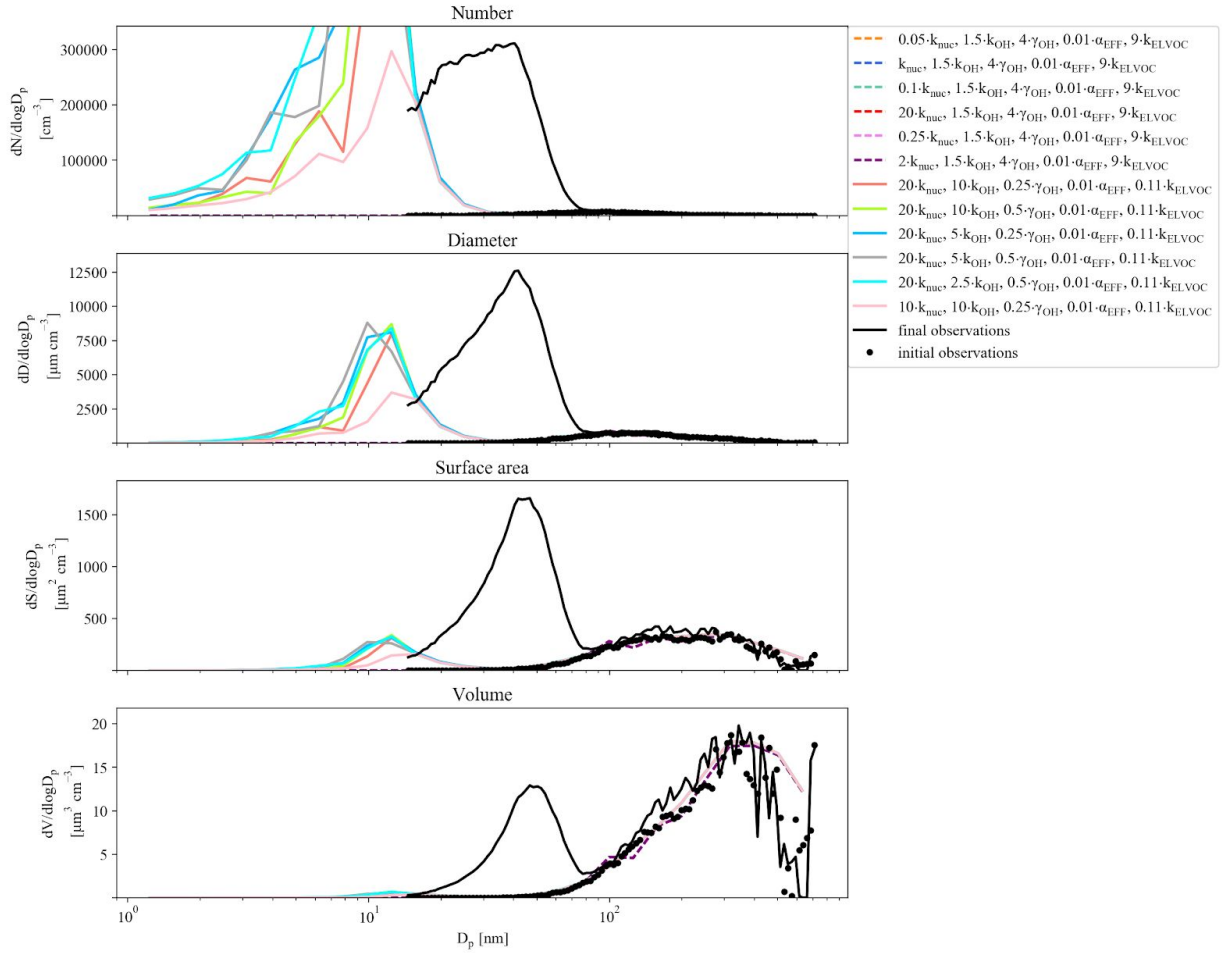

Figure S24. Example of best (solid lines) and worst (dashed lines) fit size distributions compared to the observed (black line) final OFR size distribution for a 0.53 eq days aging case from GoAmazon for the NUC1 nucleation scheme. The fits are determined using the mean error of moments method (see methods); each panel represents a separate moment. The top panel represents the number distribution; the second panel represents the diameter distribution; the third panel represents the surface area distribution; and the final (bottom) distribution represents the volume distribution. In order to see enough growth in the Aitken mode, an increase of between 20-40 times the original S/IVOC input is required. See text and Figs. 6 and S27-S33 for more details.

S7. Sensitivity of the model to the NUC2 and ACT nucleation schemes for GoAmazon

Figures S25 and S26 gives the average NME values across the 0.3-0.6 day eq. aging exposures from GoAmazon examined in this study for the parameter space that lies within the NUC2 nucleation scheme and ACT nucleation scheme, respectively, for base value of the reactive uptake coefficient. These figures use the assumption that the initial S/IVOC concentration is 30 times that of the base S/IVOC concentration (Table 2). Figure S25 is qualitatively similar to Fig. 6, which shows the same parameter space except for the NUC1 nucleation scheme. Figure S26, using the ACT nucleation scheme, shows shifted regions of best-fits as compared to the NUC1 (Fig. 6) and NUC2 (Fig. S25) nucleation schemes.

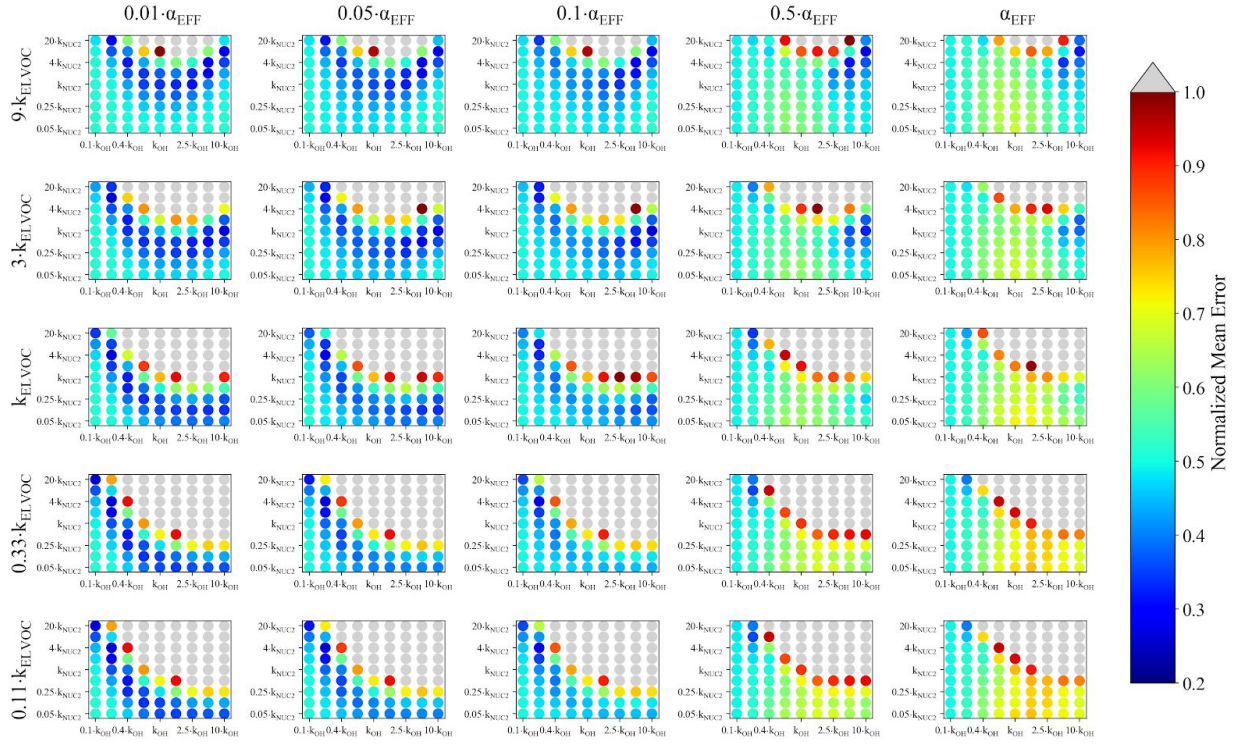

Figure S25. Representation of the parameter space for the average across the 0.3-0.6 day eq. aging exposures from GoAmazon examined in this study for the NUC2 nucleation scheme, base value of the reactive uptake coefficient of 0.6, and assumed S/IVOC concentrations of 30 times that of the baseS/IVOC concentrations. The effective accommodation coefficient increases across each row of panels; the rate constant of gas-phase fragmentation increases up each column of panels. Within each panel, the rate constant of gas-phase reactions with OH increases along the x-axis and the rate constant for nucleation increases along the y-axis. The color bar indicates the normalized mean error (NME) value for each simulation, with the lowest values indicating the least error between model and measurement. Grey regions indicate regions within the

parameter space whose NME value is greater than 1. No averaged case had a NME value less than 0.2 for the cases shown here.

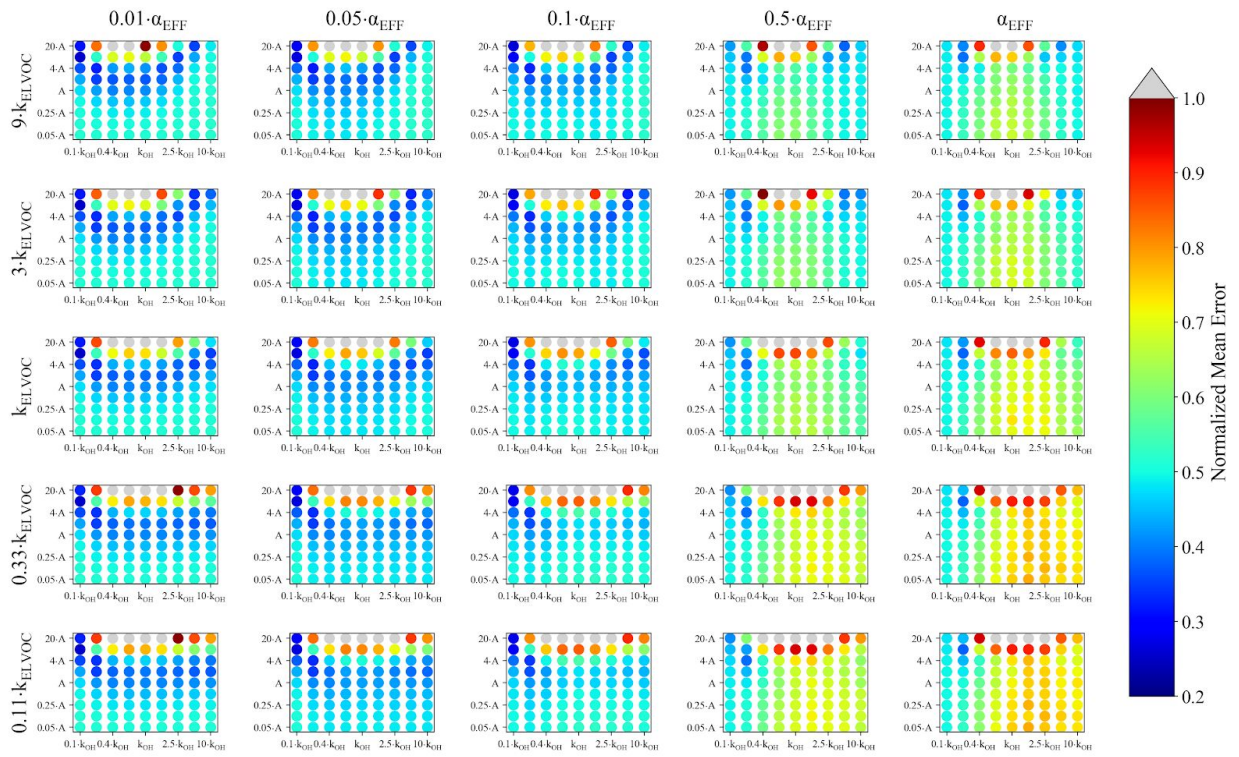

Figure S26. Representation of the parameter space for the average across the 0.3-0.6 day eq. aging exposures from GoAmazon examined in this study for the ACT nucleation scheme, base value of the reactive uptake coefficient of 0.6, and assumed S/IVOC concentration of 30 times that of the base S/IVOC concentration. The effective accommodation coefficient increases across each row of panels; the rate constant of gas-phase fragmentation increases up each column of panels. Within each panel, the rate constant of gas-phase reactions with OH increases along the x-axis and the rate constant for nucleation increases along the y-axis. The color bar indicates the normalized mean error (NME) value for each simulation, with the lowest values indicating the least error between model and measurement. Grey regions indicate regions within the parameter space whose NME value is greater than 1. No averaged case had a NME value less than 0.2 for the cases shown here.

S8. GoAmazon individual exposures and best/worst case distributions

The following are the individual representations of the model simulations for each GoAmazon exposure modelled in this study for the assumption that the initial S/IVOC concentration is 30 times that of the base S/IVOC concentration (Table 2). Figures S27, S29, S31, and S33 give the NME values for the parameter space that lies within (Table 3) the NUC1 nucleation scheme and base value of the reactive uptake coefficient. Figures S28, S30, S32, and S34 plot each observed final moment (solid black lines) used in computing the NME statistic (number, diameter, surface area, and volume) compared to the six TOMAS cases with the lowest (best) NME statistic (solid colored lines) and six TOMAS cases with the highest (worst) NME statistic (solid dotted lines). For comparison, the observed initial moments are also plotted for each moment (dotted black lines).

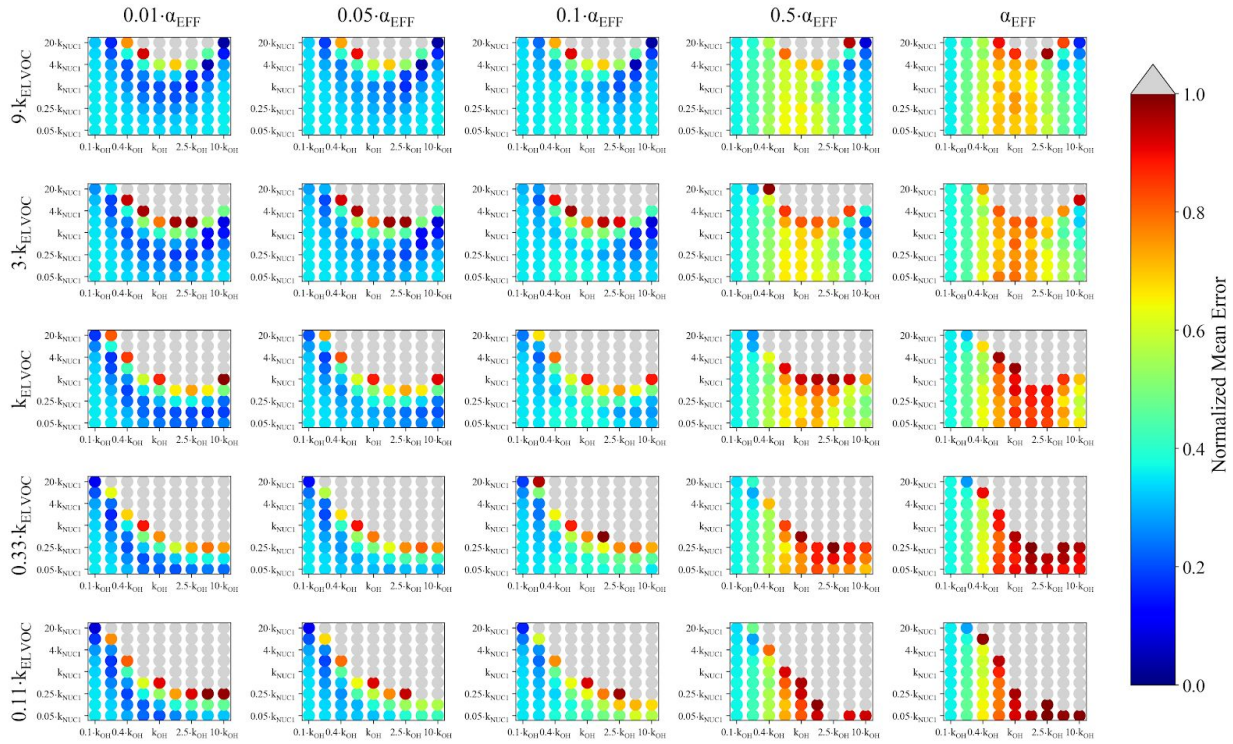

Figure S27. Representation of the parameter space for a 0.39 eq. day aging exposure from GoAmazon for the NUC1 nucleation scheme, base value of the reactive uptake coefficient of 0.6, and 30 times the base S/IVOC input concentration. The effective accommodation coefficient increases across each row of panels; the rate constant of gas-phase fragmentation increases up each column of panels. Within each panel, the rate constant of gas-phase reactions with OH increases along the x-axis and the rate constant for nucleation increases along the y-axis. The color bar indicates the normalized mean error (NME) value for each simulation, with the lowest values indicating the least error between model and measurement. Grey regions indicate regions within the parameter space whose NME value is greater than 1.

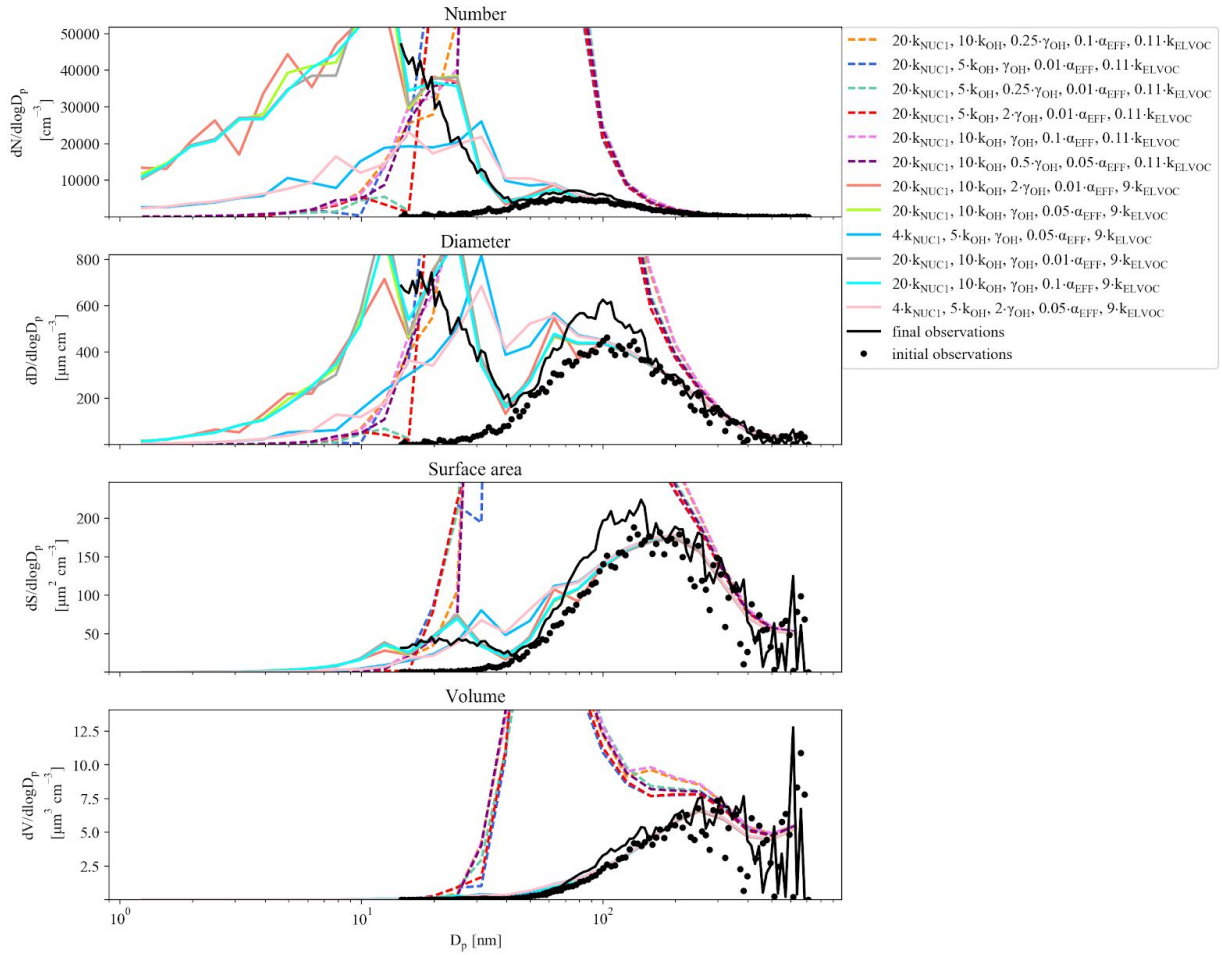

Figure S28. Example of best (solid lines) and worst (dashed lines) fit size distributions compared to the observed (black line) final OFR size distribution for a 0.39 eq. days aging case from GoAmazon for the NUC1 nucleation scheme, using 30 times the base S/IVOC input concentration. The fits are determined using the mean error of moments method (see methods); each panel represents a separate moment. The top panel represents the number distribution; the second panel represents the diameter distribution; the third panel represents the surface area distribution; and the final (bottom) distribution represents the volume distribution.

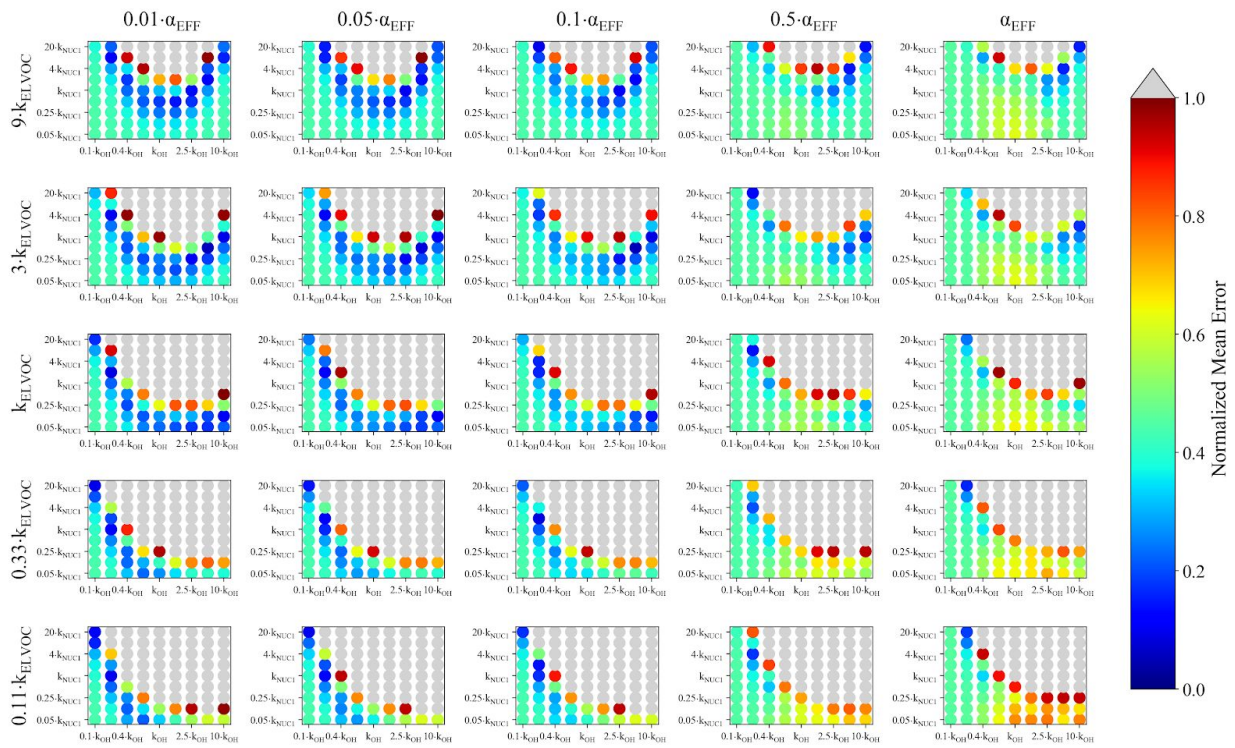

Figure S29. Representation of the parameter space for a 0.40 eq. day aging exposure from GoAmazon for the NUC1 nucleation scheme, base value of the reactive uptake coefficient of 0.6, and 30 times the base S/IVOC input concentration. The effective accommodation coefficient increases across each row of panels; the rate constant of gas-phase fragmentation increases up each column of panels. Within each panel, the rate constant of gas-phase reactions with OH increases along the x-axis and the rate constant for nucleation increases along the y-axis. The color bar indicates the normalized mean error (NME) value for each simulation, with the lowest values indicating the least error between model and measurement. Grey regions indicate regions within the parameter space whose NME value is greater than 1.

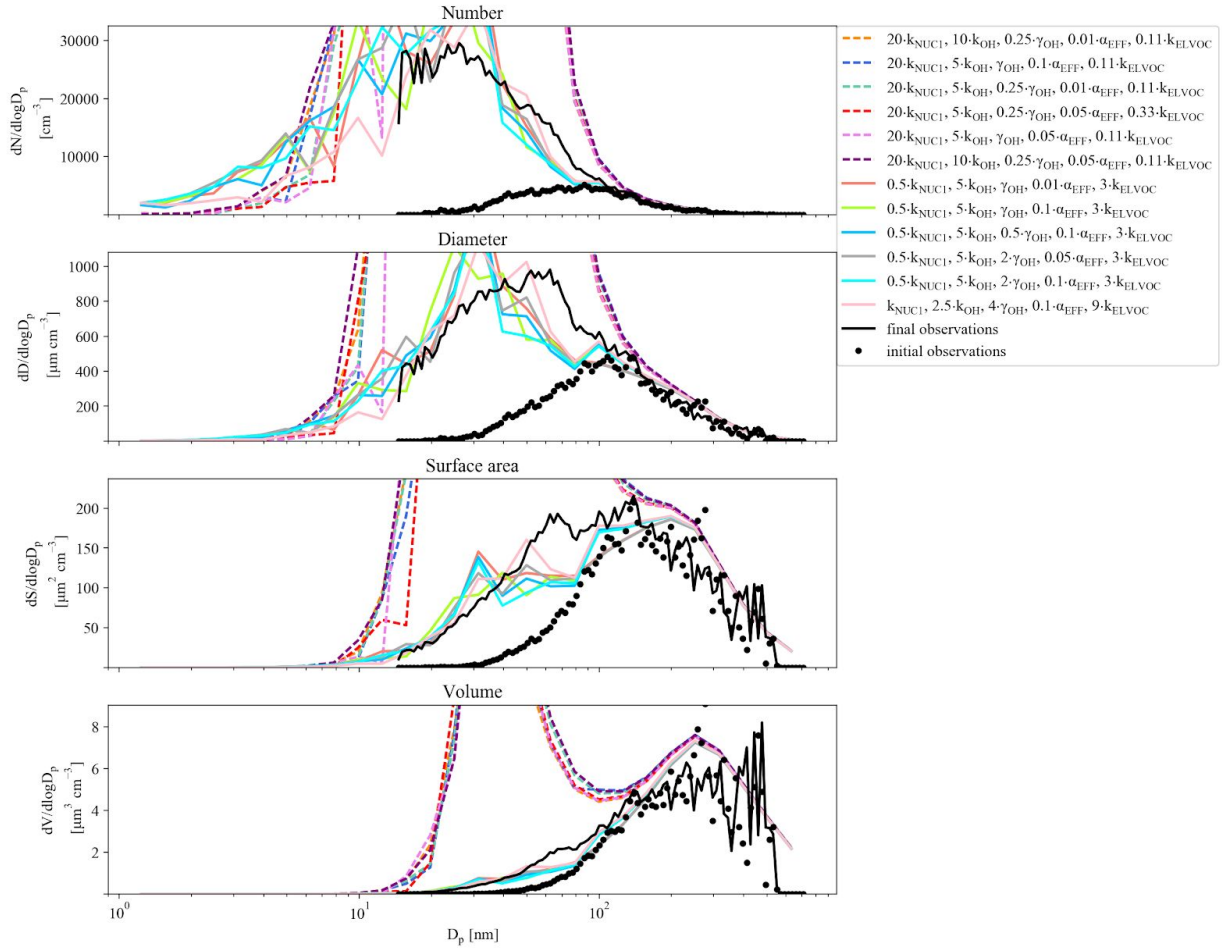

Figure S30. Example of best (solid lines) and worst (dashed lines) fit size distributions compared to the observed (black line) final OFR size distribution for a 0.40 eq days aging case from GoAmazon for the NUC1 nucleation scheme, using 30 times the base S/IVOC input concentration. The fits are determined using the mean error of moments method (see methods); each panel represents a separate moment. The top panel represents the number distribution; the second panel represents the diameter distribution; the third panel represents the surface area distribution; and the final (bottom) distribution represents the volume distribution.

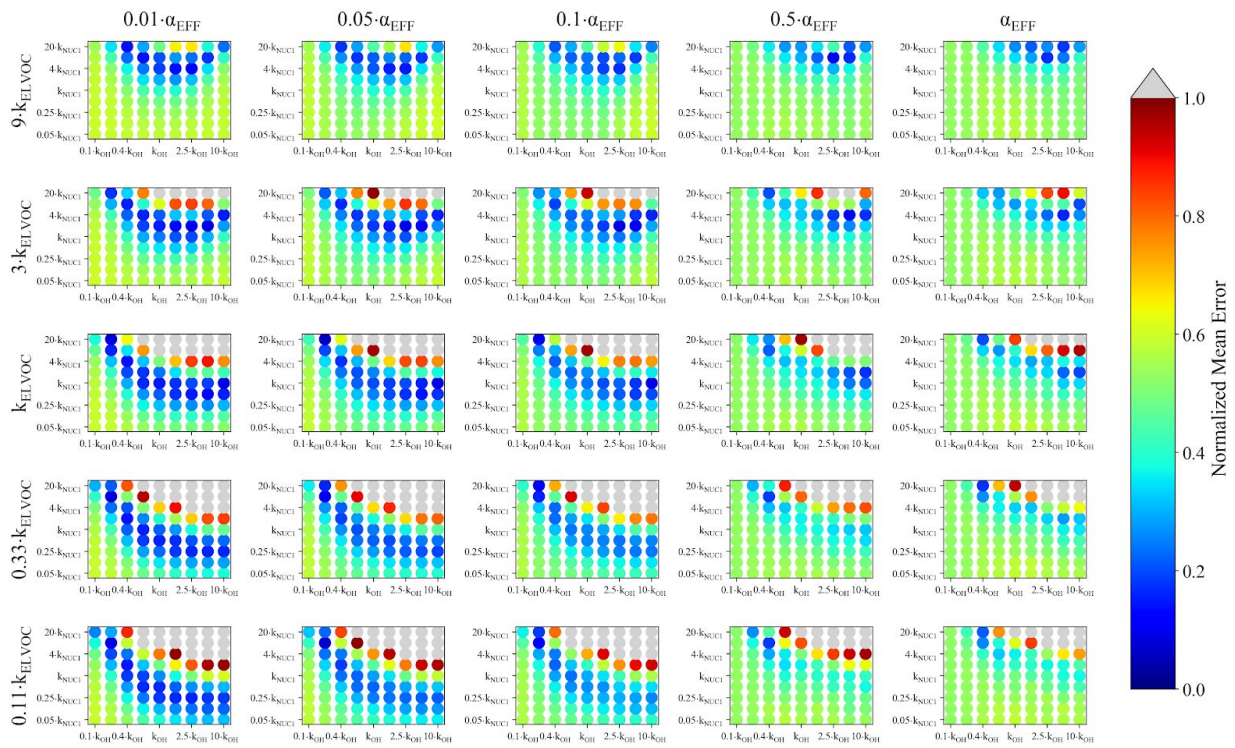

Figure S31. Representation of the parameter space for a 0.51 eq. day aging exposure from GoAmazon for the NUC1 nucleation scheme, base value of the reactive uptake coefficient of 0.6, and 30 times the base S/IVOC input concentration. The effective accommodation coefficient increases across each row of panels; the rate constant of gas-phase fragmentation increases up each column of panels. Within each panel, the rate constant of gas-phase reactions with OH increases along the x-axis and the rate constant for nucleation increases along the y-axis. The color bar indicates the normalized mean error (NME) value for each simulation, with the lowest values indicating the least error between model and measurement. Grey regions indicate regions within the parameter space whose NME value is greater than 1.

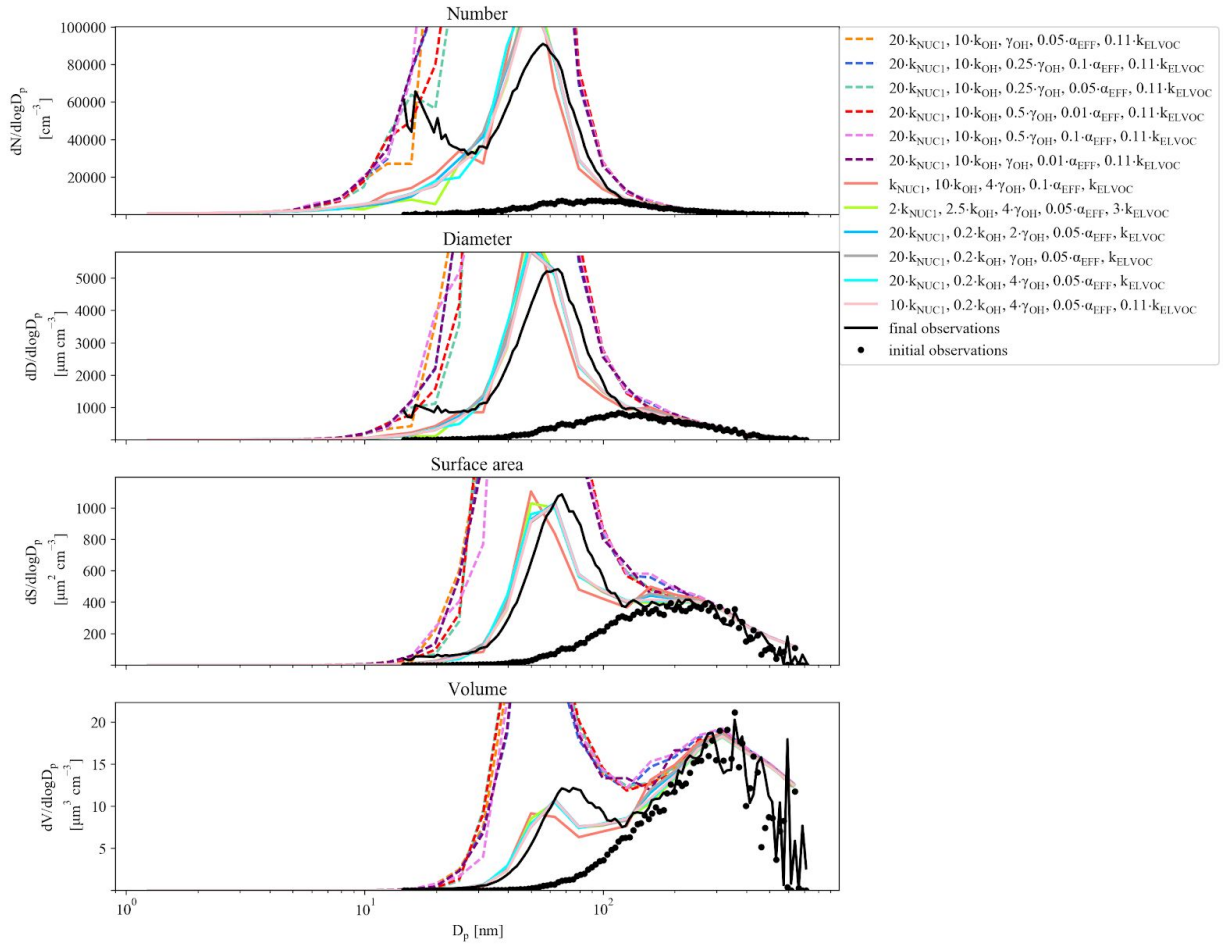

Figure S32. Example of best (solid lines) and worst (dashed lines) fit size distributions compared to the observed (black line) final OFR size distribution for a 0.51 eq days aging case from GoAmazon for the NUC1 nucleation scheme, using 30 times the base S/IVOC input concentration. The fits are determined using the mean error of moments method (see methods); each panel represents a separate moment. The top panel represents the number distribution; the second panel represents the diameter distribution; the third panel represents the surface area distribution; and the final (bottom) distribution represents the volume distribution.

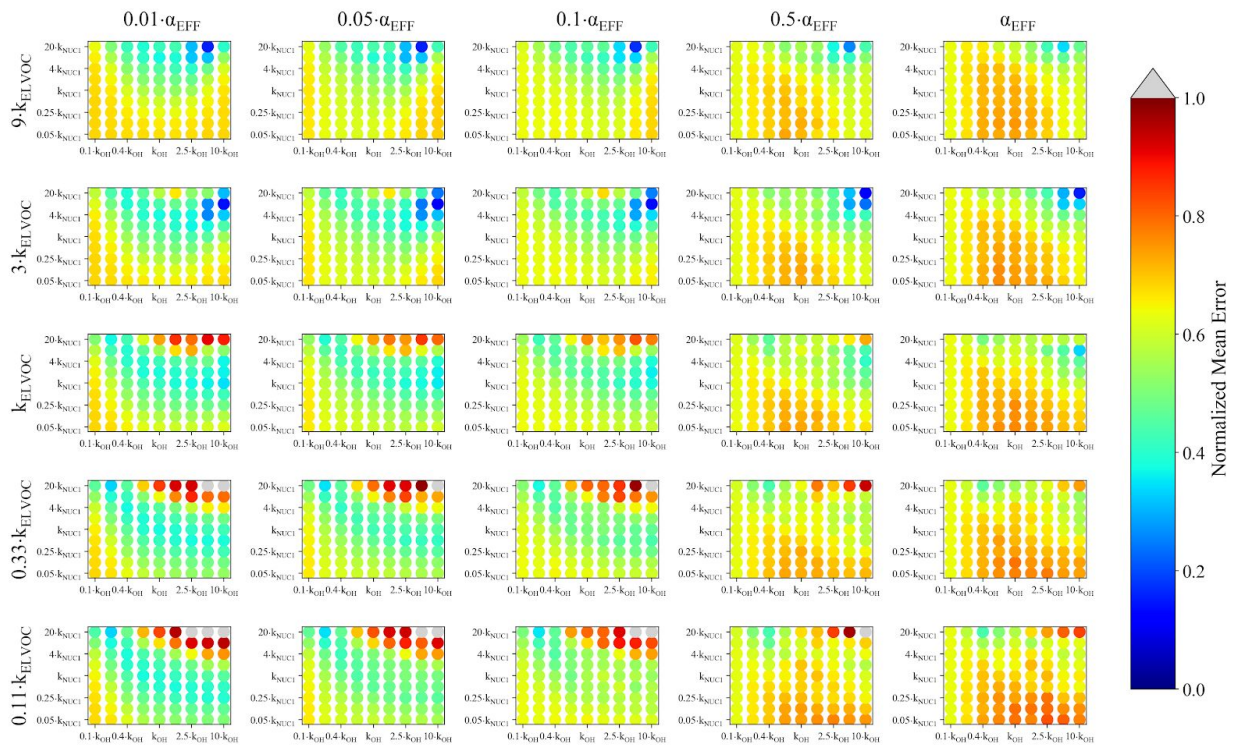

Figure S33. Representation of the parameter space for a 0.53 eq. day aging exposure from GoAmazon for the NUC1 nucleation scheme, base value of the reactive uptake coefficient of 0.6, and 30 times the base S/IVOC input concentration. The effective accommodation coefficient increases across each row of panels; the rate constant of gas-phase fragmentation increases up each column of panels. Within each panel, the rate constant of gas-phase reactions with OH increases along the x-axis and the rate constant for nucleation increases along the y-axis. The color bar indicates the normalized mean error (NME) value for each simulation, with the lowest values indicating the least error between model and measurement. Grey regions indicate regions within the parameter space whose NME value is greater than 1.

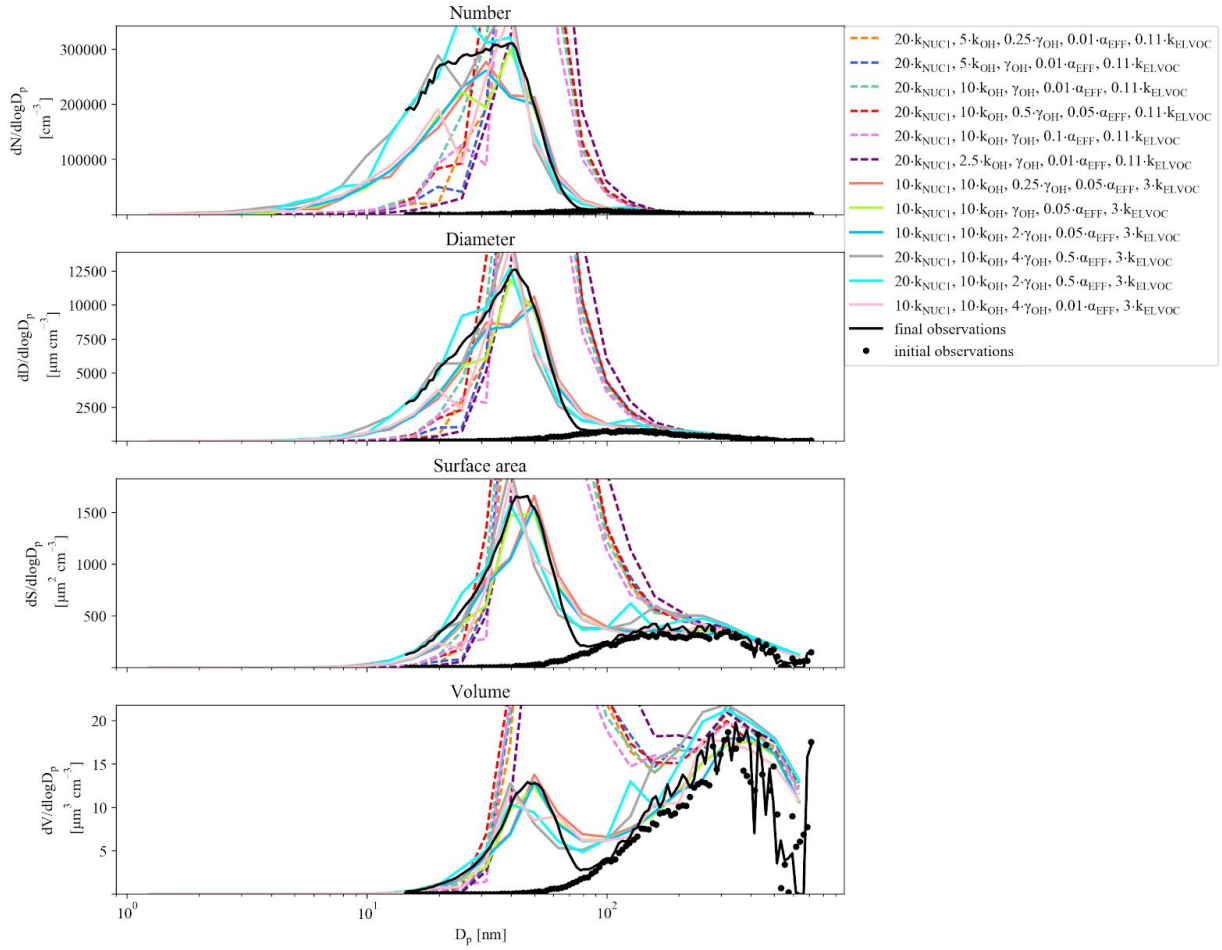

Figure S34. Example of best (solid lines) and worst (dashed lines) fit size distributions compared to the observed (black line) final OFR size distribution for a 0.53 eq days aging case from GoAmazon for the NUC1 nucleation scheme, using 30 times the base S/IVOC input concentration. The fits are determined using the mean error of moments method (see methods); each panel represents a separate moment. The top panel represents the number distribution; the second panel represents the diameter distribution; the third panel represents the surface area distribution; and the final (bottom) distribution represents the volume distribution.

References

Jathar, S. H., Donahue, N. M., Adams, P. J. and Robinson, A. L.: Testing secondary organic aerosol models using smog chamber data for complex precursor mixtures: influence of precursor volatility and molecular structure, Atmos. Chem. Phys., 14(11), 5771–5780, doi:10.5194/acp-14-5771-2014, 2014.